大阪公立大学
Osaka Metropolitan University
学術情報リポジトリ

Exchange of Nitrogen Oxides between Air and Snow in Antarctica

メタデータ	言語: eng 出版者: 公開日: 2019-06-25 キーワード (Ja): キーワード (En): 作成者: 野呂, 和嗣 メールアドレス: 所属:
URL	https://doi.org/10.24729/00000281

Exchange of Nitrogen Oxides between Air and Snow in Antarctica

（南極における大気－雪氷間の窒素酸化物交換）

Kazushi Noro

野　呂　和　嗣

February 2018

Doctoral Thesis at Osaka Prefecture University

Chapter 1: Introduction

1.1 General Introduction

Nowadays, whole human family on the planet is afflicted with environmental problems such as extinction of animals and plants, environmental pollution by hazardous chemicals, usage and disposal of radioactive materials, ozone hole, global warming, ground subsidence, acid rain, desertification, and resource shortage. For this reason, many scientists have been making efforts to preserve the global environment that humans can live comfortably through monitoring the global environment. The global environment is changing due to two reasons: anthropogenic pollution and natural dynamics. Especially changes in the global environment due to its dynamics can be known from background monitoring and paleoclimate analysis. Antarctic observation provides us the past, present and future of the global environment. This is because 1) Antarctica as the farthest place from human activities is the most suitable site for monitoring background, 2) it has simple and wide-area representation, 3) past climate record is obtained from ice core analysis, 4) it controls global climate. Furthermore, Antarctica is an observation site where scientists have paid attention, because a lot of unique phenomena specific to Antarctica such as katabatic wind, ozone hole (Solomon, 1999), temperature rise phenomenon in stratosphere, etc. have been discovered. Especially the katabatic wind is an important phenomenon greatly related to substance transportation in Antarctica (Parish, 1988). A katabatic wind originates from radiational cooling of air atop an Antarctic plateau. Antarctica has a simple shape like turning over a bowl with higher elevation inland. Since the density of air is inversely proportional to temperature, the air will flow downwards. The entire near-surface wind field over Antarctica is largely determined by the katabatic

winds, except in coastal regions when storms may impose their own wind field. In order to explore the global environment through Antarctic observation, it is indispensable to understand the Antarctic environment.

1.2 Antarctica

Antarctica is located almost entirely south of the Antarctic Circle, (66.5 degrees south Latitude). Roughly centered on the geographic South Pole (coordinates: 90° 00 S, 0° 00 E.), its total area of Antarctica is 14 million km^2 (The Columbia Encyclopedia, 6th ed.). It is the fifth largest continent, following Asia, Africa, North America, and South America, containing 8.9% of the Earth's land area; and it is larger than Australia and the subcontinent of Europe. The first Byrd Expedition to the South Pole was during the years 1928-1930. Following World War II, there was an upsurge in scientific research on the continent. A number of countries have set up year-round research stations on Antarctica. Seven have made territorial claims, but not all countries recognize these claims. In order to form a legal framework for the activities of nations on the continent, an Antarctic Treaty was negotiated that neither denies nor gives recognition to existing territorial claims; signed in 1959, it entered into force in 1961. Antarctica is the coldest, windiest, harshest continent, and with little precipitation is the driest place on earth. It has an average elevation of higher than 2000 m, and 98% of the landmass is covered by an ice sheet estimated to be 29 million km^3. For example, the average annual temperature at Dome Fuji Station and Showa station are −54.4 and −10.5 °C, respectively. In addition, weather conditions across the Antarctic are simulated (Zatko *et al.*, 2016). Fig. 1 shows

the simulated weather conditions comparing with Greenland; (a,b): Temperature; (c,d): Accumulation rate; and (e,f): Wind divergence. Inland area of Antarctica is characterized by low temperature and low accumulation rate comparing to Greenland and Antarctic costal site. On the other hand, there is a strong wind blowing between domes and the coastal area which is called katabatic wind.

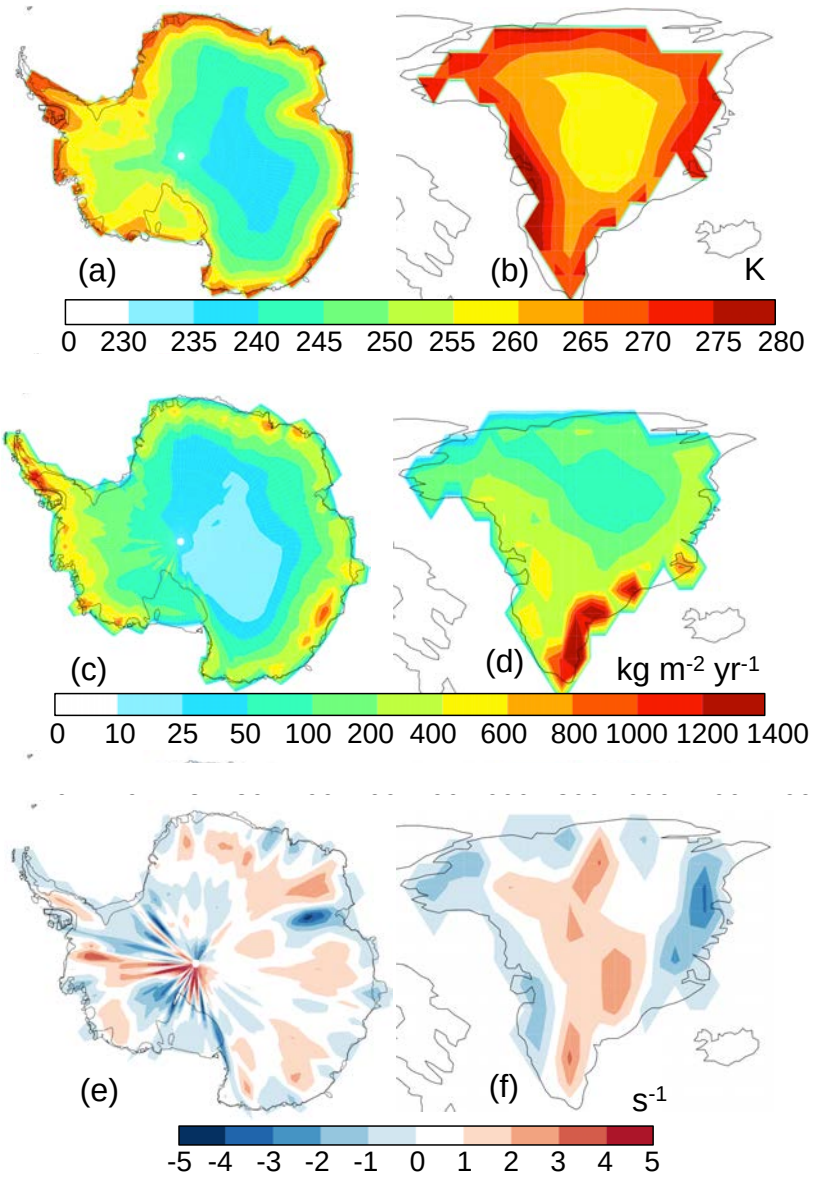

Fig.1 Weather conditions in Antarctica and Greenland (taken from Zatko et al., 2016)

Beneath its thick ice sheets, Antarctica is a dynamic and diverse continent with mountains, volcanoes, deserts, meteorites, dinosaur fossils, and some of the Earth's most ancient crust. Being the coldest and windiest continent, Antarctica exhibits severe low temperatures that vary with latitude, elevation, and distance from the ocean. East Antarctica is colder than West Antarctica because of its higher elevation. Much research is being conducted on the climatology and meteorology of Antarctica because the conditions here are thought to have an enormous impact on climate patterns on the rest of the planet. There is also much interest in examining how both natural and anthropogenic changes in earth's climate are affecting the ice and biological processes. Because Antarctica contains 90% of earth's ice and 70% of its freshwater, any changes in temperature could cause the ice to melt and raise the world-wide sea level. The circumpolar ocean current, travels from west to east off the coast, effectively isolating the continent from the warmer ocean currents to the north. Upwelling of water provides not only nutrients that support a rich variety of ocean life, but provides a contact point for the ocean and the atmosphere to meet so that carbon dioxide can be absorbed.

1.3 Antarctic Ice Core

Antarctica provides a wonderful laboratory to examine the historical patterns of earth's climate. Ice cores taken have enables scientists to peer back 740,000 years in time to analyze the chemistry of earth's atmosphere and to estimate the average temperatures (Abram, Wolff, & Curran, 2013; Caiazzo *et al.*, 2016; Felix & Elliott, 2013; Fischer *et al.*, 2013; Grannas *et al.*, 2006; Hastings *et al.*, 2004; Hastings, Jarvis, & Steig, 2009; Petit *et*

al., 1999; Sofen *et al.*, 2014). Glaciers form in polar areas as snow falls and accumulates. Basically, the chemical components deposited in the snowpack represent the atmospheric chemical compositions of the deposition age. The thickness of a year's snow accumulation at the surface must be identical to the precipitation rate. However, its thickness changes by its own weight when snow transforms into glacier. It preserves wealth information with a variety proxies. The primary record in ice core is paleo temperature recorded in the ice as $\delta^{18}O$ or δD of water. This calculation utilizes isotopic mass fractionation theory in water phase transition. Not only the past temperature but also the past atmospheric composition can be reconstructed from the ice core analysis. There are reports that the ice core record of nitrate in Greenland offers a means to track changes in NO_x sources through time (Hastings *et al.*, 2009). Nitrogen oxides play a key role in controlling the concentrations of atmospheric oxidants that drive tropospheric chemistry. Sources of NO_x are both of natural (e.g. lightning, soil nitrification / denitrification, and wildfires) and anthropogenic (e.g. fossil fuel combustion, industry, and agricultural) origin (Walters *et al.*, 2015), however, there are uncertainties in the temporal and spatial contributions of various emission sources that might be resolved by stable isotope analysis.

1.4 Nitrogen Cycle

Nitrogen is an essential element for life (Nitrogen oxides dictionary, 2008). It is an important component of DNA, RNA and proteins, a building blocks of life, and necessary for all creatures to grow alive (Galloway & B Cowling, 2002). Nearly 80 % of the

atmospheric total mass consists of N_2, while N_2 is biologically almost unavailable to living organisms due to the strong triple bond between the N atoms (Galloway & B Cowling, 2002). As breaking this triple bond is a high energy reaction, it is more chemically available of N, such as ammonium (NH_4^+), nitrate (NO_3^-), and organic nitrogen which are converted from N_2 by only a few species of microorganism to fix. The fixed N is very versatile both in organic and inorganic forms as well as in many oxidation states (+5 for NO_3^- to −3 for NH_3). Transportation of N between different forms of atmosphere, biosphere and geosphere is described by nitrogen cycle, one of the major biogeochemical cycle on the Earth. Throughout the nitrogen cycle, N undergoes different redox reactions through the main process of nitrogen fixation, nitrogen assimilation, mineralization, nitrification and denitrification (Nitrogen oxides dictionary, 2008). As a microbial-mediated process, the rate of transformation depends on the environmental factors controlling the microbial community, such as temperature, moisture, pH and the availability of resources. Negative impact of urban activities including increment of pollutants such as reactive nitrogen oxides (NO_y: NO, NO_2 and HONO) may cause the secondary pollutants formation (O_3 and particulate matter). NO_y is released from various sources (anthropogenic is dominant), being converted between NO and NO_2 by (R1, 2 and 3).

$$NO + O_3 \rightarrow NO_2 + O_2 \quad \text{(R1)}$$

$$NO + HO_2 \text{ (or ROO)} \rightarrow NO_2 + OH \text{ (or RO)} \quad \text{(R2)}$$

$$NO_2 + h\nu \rightarrow NO + O \quad \text{(R3)}$$

The production of HNO_3 is the main sink of NO_y in the atmosphere. NO_2 reacts with OH to form HNO_3 (R4). NO_3 is formed by the reaction of NO_2 and O_3 (R5). Formed NO_3 reacts with NO_2 to form dinitrogen pentoxide (R6), which forms $2HNO_3$ with water on surface (R7).

$$NO_2 + OH + M \rightarrow HNO_3 + M \qquad \text{(R4)}$$

$$NO_2 + O_3 \rightarrow NO_3 + O_2 \qquad \text{(R5)}$$

$$NO_2 + NO_3 \rightleftharpoons N_2O_5 \qquad \text{(R6)}$$

$$N_2O_5 + H_2O + \text{surface} \rightarrow 2HNO_3 \qquad \text{(R7)}$$

Gaseous HNO_3 is highly water soluble and sticky, therefore, easily deposited by wet or dry deposition. The NO_y removal changes the mixing ratios of O_3 and OH with affecting aerosol generation. In addition, HONO also plays significant role to the atmospheric processes as one dominant source of OH radical (R8) (Alicke *et al.*, 2003; Alicke, Platt, & Stutz, 2002; Czader *et al.*, 2012; Kleffmann & Wiessen, 2008; Li *et al.*, 2010; Ren *et al.*, 2003; Spataro & Ianniello, 2014; Stockwell & Calvert, 1978; Stutz *et al.*, 2000). In the gas phase, HONO produced from nitrate photolysis is a trace amount, however, in the ice phase HONO is the main product (R9, 10).

$$HONO + h\nu \rightarrow NO + OH \qquad \text{(R8)}$$

$$HNO_3\,(\text{ads}) + h\nu \rightarrow HONO + O\,(\text{ads}) \qquad \text{(R9)}$$

$HNO_3 \cdot H_2O + h\nu \rightarrow HONO + H_2O_2$ (R10)

These nitrogen oxides have been measured in various ways. HNO_3 gas has been measured by denuder method or filter pack method. NOx is measured by absorption photometry with Zalzmann reagent, chemiluminescence and cavity attenuated phase shift (CAPS) method. Because HONO has properties similar to NO_2 of which concentration is generally 20 times higher than HONO concentration. Thus, it is difficult to perform accurate measurement of HONO. HONO has been measured by different techniques, including: optical spectroscopic methods (differential optical absorption spectroscopy (DOAS) (Platt *et al.*, 1980), tunable infrared laser absorption spectroscopy (Schiller *et al.*, 2001), photo-fragmentation/laser-induced fluorescence (Rodgers & Davis, 1989), wet chemical methods (wet effluent diffusion denuder (Vecera & Dasgupta, 1991), mist chamber-IC, HPLC/UV system (Zhou *et al.*, 1999), long-path absorption photometric technique (LOPAP) (Heland *et al.*, 2001; Kleffmann & Wiesen, 2008), air-dragged aqua-membrane denuder (ADAMD)-fluorescence detector (Takenaka *et al.*, 2004) and other off-line methods.

1.5 Isotopic Analysis

Isotopic ratio in nature seems to be uniform at first glance, in fact, it may fluctuate under various process in nature. Therefore, it is useful to estimate the global material cycle and the physicochemical / biological environment of elements by its isotopic ratio. On the earth, isotope fractionation occurs mainly due to radiation decay, physicochemical

fractionation, and biological processes. Radioactive disintegration occurs at a certain rate, physicochemical fractionation and biological fractionation occur depending on mass, thus these isotope fluctuations lead to geochemically important information as described below. In addition, mass independent fractionation (MIF) have also been found recently. Some of isotopes in natural are radiogenic which emit α, β or γ ray to be stable. By using this radiation decays it is possible to determine the age of rocks and minerals, and apply to the monitoring of material cycle on a global scale. It is known that the decreasing rate of isotopes causing radiation decay is proportional to the existing number (N) of the isotopes.

$$-\mathrm{d}N/\mathrm{d}t \propto N \qquad \text{(R11)}$$

The proportionality constant in the above equation is called a disintegration constant (λ), and the above equation can be rewritten as follows;

$$-\mathrm{d}N/\mathrm{d}t = \lambda N \qquad \text{(R12)}$$

When it is integrated as follows;

$$N = N_0 \mathrm{e}^{-\lambda t} \qquad \text{(R13)}$$

N_0 is an initial value. In other words, the isotope causing radiation decay decrease

exponentially with time. The disintegration constant λ is determined by the isotope that causes radiation decay. For example, ^{87}Rb beta decays to ^{87}Sr with a disintegration constant 1.42×10^{-11} (year^{-1}) (half life: 48.8 billion years). It has been used for dating the rock samples on the earth, moonrocks and meteorites. In addition, dating using radiative decay systems such as ^{40}K-^{40}Ar, ^{147}Sm-^{143}Nd, ^{238}U-^{206}Pb, ^{235}U-^{207}Pb, ^{232}Th-^{208}Pb are commonly used in earth science research fields.

Isotopes of different mass have different physicochemical properties due to isotope effect. For example, the melting point of water differs by 3.8 °C for light water and heavy water. The isotope effect appears more conspicuously as the mass difference relative to mass, hydrogen is most strongly isotope fractionated, and boron, carbon, nitrogen, oxygen, silicon, sulfur, chlorine isotope fractionations have been well known. Recently, due to advances in analytical techniques, even heavier elements such as magnesium, calcium, iron, copper, and tin have also been focused. Isotope mass dependent fractionation in nature depends on isotope effect, however, in the natural environment where both movement and reaction occur, it is necessary to consider the following three stages. First is isotope exchange reaction, secondly reaction rate, thirdly molecular diffusion. Firstly, isotope exchange reaction due to the difference in stability of molecules between in two different molecules is an equilibrium phenomena. For example, in the next reaction, the free energies of reactions are different between right and left directions. The right side is slightly more stable.

$$H_2{}^{18}O + 1/2C^{16}O_2 \rightleftharpoons H_2{}^{16}O + 1/2C^{18}O_2 \quad \text{(R14)}$$

Secondary, the difference in reaction rate is a kinetic phenomenon. Potential energy of bonds with heavier isotopes is higher than bonds with lighter isotopes, then reaction rate becomes lower. Thirdly, in molecular diffusion, for example in the case of a gas molecule, the average velocity of the molecule is inversely proportional to the root of the molecular weight. Therefore, light molecules can spread or move faster than heavier molecules. The third effect is observed only in closed systems. These three different isotopic effects occur overlapping in nature. It often makes analysis difficult, however on the contrary, the cycle may be estimated from analyzing which effects are dominant. In common with these three causes, the fractionation is almost proportional to the mass difference. For example, plotting ^{17}O / ^{16}O and ^{18}O / ^{16}O for all the substances on the earth line up on a line (Terrestrial Fractionation Line: TFL) (Fig. 2), however the Martian meteorites constitute a straight line with the same slope but different intercept.

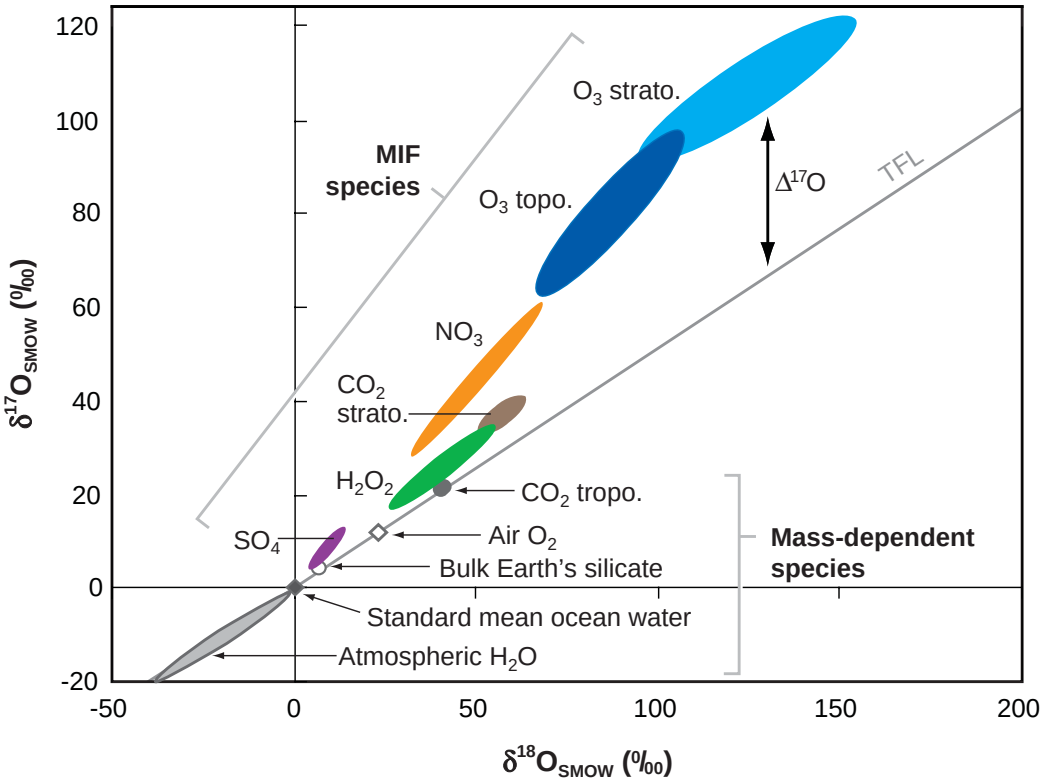

Fig. 2 Oxygen isotopic composition of atmospheric species (taken from Thiemens 2006)

The moon samples are plotted on the same line as the Earth. This indicates that the moon has material origin in common with the earth (Clayton, Grossman, & Mayeda, 1973). Moreover, the definitive evidence that the meteorite with the existence of life is derived from Mars was made by measuring the oxygen isotopic ratio (Clayton & Mayeda, 1996). MIF is found from O_3, CO_2, N_2O, CO molecules in the Earth's atmosphere or oxygen isotopic ratios of carbonate minerals in Martian origin meteorites. In the case of "mass-dependent isotopic fractionation" caused by ordinary physicochemical processes,

oxygen isotopes fluctuate on the TFL, while when ozone is generated from oxygen molecules, the product ozone and the isotope of the oxygen molecule of the unreacted substance is separated from the TFL (Thiemens, 2001). As for the mechanism of MIF, for example in the case of ozone, differences in stability derived from asymmetry of molecular species such as $^{16}O^{16}O^{17}O$ or $^{16}O^{16}O^{18}O$ to $^{16}O^{16}O^{18}O$ is mentioned. The governing premise was that the lifetime of the excited state O_3^* molecule, immediately formed during an oxygen atom-molecule collision, is enhanced for the asymmetric species with respect to the symmetric. This enhanced lifetime arises owing to the doubling of the asymmetric states ($^{16}O^{16}O^{17}O$, $^{16}O^{16}O^{18}O$) with respect to the symmetric states $^{16}O^{16}O^{16}O$, which provide a more effective energy distribution. This was the first suggestion that symmetry factors are of importance in an isotopic fractionation process for ozone formation. In addition, MIF has been found for sulfur isotopes by photo-polymerization in the gas phase (Farquhar, Bao, & Thiemens, 2000).

Nitrogen and oxygen isotopes of nitrate have been used to estimate the nitrogen cycle. Nitrogen has two stable isotopes with mole fractions of: ^{14}N (0.9963) and ^{15}N (0.0037) whereas oxygen has three stable isotopes: ^{16}O (0.9976), ^{17}O (0.0004) and ^{18}O (0.0020). Due to the abundance of stable isotopes is very small, analytical techniques have been established to measure relative intensities with standards. Thus, isotopic composition of sample (x) and standard (std) in terms of dimensionless δ value is defined as below;

$$\delta_x = (R_x / R_{std} - 1) \times 1000 \quad \text{(R15)}$$

where R is the ratio of the rare isotope to the abundant isotope. The standard of nitrogen and oxygen are N_2 gas in the atmosphere and Vienna Standard Mean Ocean Water, respectively (Coplen *et al.*, 2002). The use of triple oxygen isotopic analysis to gain further insights into biogeochemistry research is a significant advancement recently. A nearly linear relationship between $\delta^{17}O$ and $\delta^{18}O$ (Miller, 2002) is expressed as $\delta^{17}O = 0.52 \times \delta^{18}O$. Then, MIF is denoted by $\Delta^{17}O$ and can be quantified by Miller (2002) (Fig. 1):

$$\Delta^{17}O = \delta^{17}O - 0.52 \times \delta^{18}O \quad \text{(R16)}$$

Nitrate ($HNO_3(g)$ + p-NO_3^-) is one of the final oxidation products of reactive nitrogen species (NO_y: NO, NO_2 and HONO) in the atmosphere; it is also one of the major ions found in polar ice cores. Therefore, nitrate in ice cores is a potential proxy for NO_y levels in the atmosphere of the past (Dibb *et al.*, 1998). However, nitrate in Antarctic snow or ice core is lost by post-depositional process (Jones *et al.*, 2001; Davis *et al.*, 2004; Meusinger *et al.*, 2014; Zatko *et al.*, 2013) thus it is difficult to track its origin. Recently, a chemical model of nitrate behavior at the air–snow interface on the East Antarctic Plateau has been developed (Zatko *et al.*, 2016), to reconstruct $\Delta^{17}O(NO_3^-)$ values in the atmosphere. The determination of past atmospheric $\Delta^{17}O(NO_3^-)$ values from ice core

analysis, coupled with global atmospheric chemical transport model such as GEOS-Chem, which quantify atmospheric nitrate formation pathways (Alexander *et al.*, 2009), provides the scope for reconstructing past atmospheric oxidizing capacity and its relationship to past global changes.

1.6 Optical Snow Property

It is also important to understand the optical properties of snow to elucidate the nitrate post-depositional process. Speaking of the optical properties of snow, albedo has been measured and modeled by many researchers. Over Antarctica snow albedo averages a little more than 0.8. If a marginally snow-covered area warms, snow tends to melt, lowering the albedo, and hence leading to more snowmelt because more radiation is being absorbed by the snowpack. The albedo changes the thermal energy received by the Earth, affecting greatly the global energy balance. Although attention has been paid to the light reflected on the snow, less attention has been paid to the light penetrated into the snow. There are no reports on light multiple scattering within snowpack, the influence on the spectrum of light. In a similar case, it is well known that holes digged into pure snowpack are glowing blue. This phenomenon is due to the absorption of long wave length light of visible light by water molecules just like the blue sea.

1.7 Subject of This Thesis

Based on these background, this study focused on the Antarctic nitrogen oxide Cycle, especially the nitrate photolysis mechanism in snowpack and its products. This thesis

consists of the five chapters. Chapter 1 described background. In chapter 2, in order to elucidate the post-depositional process of nitrate in the Antarctic snowpack, nitrogen and oxygen isotopic ratios of nitrate in surface snow collected from coastal to inland in East Antarctica was reported. In chapter 3, NO_y flux observed in summer Antarctic coast and vertical profile of NO_y in firn were reported. The composition of the NO_y flux was NO: HONO: NO_2 = 2: 1: 0. This result is considered to contribute to improvement of accuracy of Antarctic atmospheric chemistry model. In chapter 4, it is reported that nitrate photolysis experiment with uniform snow in summer Antarctic coastal area. Knowledge on the post-depositional loss of nitrate by laboratory experiments is insufficient. In particular, it is very difficult to reproduce the Antarctic conditions. Therefore, in order to investigate the post-depositional process in detail, nitrate photolysis experiment in a glass tube with mixed natural snow was conducted in summer Antarctic coastal area. In chapter 5, an overview of the thesis and the prospects for the future are described.

References

Abram, N. J., Wolff, E. W. and Curran, M. A. J. (2013). A review of sea ice proxy information from polar ice cores. *Quaternary Sci. Rev., 79*, 168-183. doi:10.1016/j.quascirev.2013.01.011

Alexander, B., Hastings, M. G., Allman, D. J., Dachs, J., Thornton, J. A. and Kunasek, S. A. (2009). Quantifying atmospheric nitrate formation pathways based on a global model of the oxygen isotopic composition ($\Delta^{17}O$) of atmospheric nitrate. *Atmos. Chem. Phys., 9*(14), 5043-5056. doi:10.5194/acp-9-5043-2009

Alicke, B., Geyer, A., Hofzumahaus, A., Holland, F., Konrad, S., Pätz, H. W., Schäfer, J., Stutz, J., Volz-Thomas, A. and Platt, U. (2003). OH formation by HONO photolysis during the BERLIOZ experiment. *J. Geophys. Res.-Atmos., 108*(D4). doi:10.1029/2001JD000579

Alicke, B., Platt, U. and Stutz, J. (2002). Impact of nitrous acid photolysis on the total hydroxyl radical budget during the Limitation of Oxidant Production/Pianura Padana Produzione di Ozono study in Milan. *J. Geophys. Res.-Atmos., 107*(D22). doi:10.1029/2000JD000075

Caiazzo, L., Becagli, S., Frosini, D., Giardi, F., Severi, M., Traversi, R. and Udisti, R. (2016). Spatial and temporal variability of snow chemical composition and accumulation rate at Talos Dome site (East Antarctica). *Sci. Total Environ., 550*, 418-430. doi:10.1016/j.scitotenv.2016.01.087

Clayton, R. N., Grossman, L. and Mayeda, T. K. (1973). A Component of Primitive

Nuclear Composition in Carbonaceous Meteorites. *Science, 182*(4111), 485-488. doi:10.1126/science.182.4111.485

Clayton, R. N. and Mayeda, T. K. (1996). Oxygen isotope studies of achondrites. *Geochim. Cosmochim. Acta, 60*(11), 1999-2017. doi:https://doi.org/10.1016/0016-7037(96)00074-9

Coplen, T. B., Hopple, J. A., Bohlke, J., Peiser, H. S., Rieder, S. E., Krouse, H. R., Rosman, K. J. R., Ding, T., Vocke, Jr., R. D., Révész1, K. M., Lamberty, A., Taylor, P. and De Bièvre, P. (2002). Compilation of Minimum and Maximum Isotope Ratios of Selected Elements in Naturally Occuring Terrestrial Materials and Reagents. U.S. Geological Survey Water-Resources Investigations Report 01-4222.

Czader, B. H., Rappenglück, B., Percell, P., Byun, D. W., Ngan, F. and Kim, S. (2012). Modeling nitrous acid and its impact on ozone and hydroxyl radical during the Texas Air Quality Study 2006. *Atmos. Chem. Phys., 12*(15), 6939-6951. doi:10.5194/acp-12-6939-2012

Davis, D., Chen, G., Buhr, M., Crawford, J., Lenschow, D., Lefer, B. and Hogan, A. (2004). South Pole NOx Chemistry: an assessment of factors controlling variability and absolute levels. *Atmos. Environ., 38*(32), 5375-5388. doi:https://doi.org/10.1016/j.atmosenv.2004.04.039

Dibb, J. E., Talbot, R. W., Munger, J. W., Jacob, D. J. and Fan, S.-M. (1998). Air-snow exchange of HNO_3 and NO_y at Summit, Greenland. *J. Geophys. Res.-Atmos., 103*(D3), 3475-3486. doi:10.1029/97JD03132

Farquhar, J., Bao, H. and Thiemens, M. (2000). Atmospheric Influence of Earth's Earliest

Sulfur Cycle. *Science, 289*(5480), 756-758. doi:10.1126/science.289.5480.756

Felix, J. D. and Elliott, E. M. (2013). The agricultural history of human-nitrogen interactions as recorded in ice core $\delta^{15}N\text{-}NO_3^-$. *Geophys. Res. Lett., 40*(8), 1642-1646. doi:10.1002/grl.50209

Fischer, H., Severinghaus, J., Brook, E., Wolff, E., Albert, M., Alemany, O. and Wilhelms, F. (2013). Where to find 1.5 million yr old ice for the IPICS "Oldest-Ice" ice core. *Climate of the Past, 9*(6), 2489-2505. doi:10.5194/cp-9-2489-2013

Galloway, J. and B Cowling, E. (2002). *Reactive Nitrogen and The World: 200 Years of Change. Ambio, 31(2),* 64-71.

Grannas, A. M., Hockaday, W. C., Hatcher, P. G., Thompson, L. G. and Mosley-Thompson, E. (2006). New revelations on the nature of organic matter in ice cores. *J. Geophys. Res.-Atmos., 111*(D4), D04304. doi:10.1029/2005JD006251

Hastings, M. G., Jarvis, J. C. and Steig, E. J. (2009). Anthropogenic impacts on nitrogen isotopes of ice-core nitrate. *Science, 324*(5932), 1288. doi:10.1126/science.1170510

Hastings, M. G., Steig, E. J. and Sigman, D. M. (2004). Seasonal variations in N and O isotopes of nitrate in snow at Summit, Greenland: Implications for the study of nitrate in snow and ice cores. *J. Geophys. Res.-Atmos., 109*(D20). doi:10.1029/2004JD004991

Heland, J., Kleffmann, J., Kurtenbach, R. and Wiessen, P. (2001). A New Instrument To Measure Gaseous Nitrous Acid (HONO) in the Atmosphere. *Environ. Sci. Technol., 35*(15), 3207-3212. doi:10.1021/es000303t

Jones, A. E., Weller, R., Anderson, P. S., Jacobi, H. W., Wolff, E. W., Schrems, O. and Miller, H. (2001). Measurements of NOx emissions from the Antarctic snowpack. *Geophys. Res. Lett., 28*(8), 1499-1502. doi:10.1029/2000GL011956

Kleffmann, J. & Wiessen, P. (2008). Technical Note: Quantification of interferences of wet chemical HONO LOPAP measurements under simulated polar conditions. *Atmos. Chem. Phys., 8*(22), 6813-6822. doi:10.5194/acp-8-6813-2008

Li, G., Lei, W., Zavala, M., Volkamer, R., Dusanter, S., Stevens, P. and Molina, L. T. (2010). Impacts of HONO sources on the photochemistry in Mexico City during the MCMA-2006/MILAGO Campaign. *Atmos. Chem. Phys., 10*(14), 6551-6567. doi:10.5194/acp-10-6551-2010

Meusinger, C., Berhanu, T. A., Erbland, J., Savarino, J. and Johnson, M. S. (2014). Laboratory study of nitrate photolysis in Antarctic snow. I. Observed quantum yield, domain of photolysis, and secondary chemistry. *J. Chem. Phys., 140*(24), 244305. doi:10.1063/1.4882898

Miller, M. (2002). Isotopic fractionation and the quantification of ^{17}O anomalies in the oxygen three-isotope system: An appraisal and geochemical significance. *Geochim. Cosmochim. Ac., 66(11),* 1881-1889. doi.org/10.1016/S0016-7037(02)00832-3

Parish, T. R. (1988). Surface winds over the Antarctic continent: A review. *Reviews of Geophysics, 26*(1), 169-180. doi:10.1029/RG026i001p00169

Petit, J. R., Jouzel, J., Raynaud, D., Barkov, N. I., Barnola, J. M., Basile, I., Basile, I., Bender M., Chappellaz, J., Davis, M., Delaygue, G., Delmotte, M., Kotlyakov, V.

M., Legrand, M., Lipenkov, V. Y., Lorius, C., PÉpin, L., Ritz, C., Saltzman, E. and Stievenard, M. (1999). Climate and atmospheric history of the past 420,000 years from the Vostok ice core, Antarctica. *Nature, 399*, 429-436. doi:10.1038/20859

Platt, U., Perner, D., Harris, G. W., Winer, A. M. and Pitts Jr, J. N. (1980). Observations of nitrous acid in an urban atmosphere by differential optical absorption. *Nature, 285*, 312. doi:10.1038/285312a0

Ren, X., Harder, H., Martinez, M., Lesher, R. L., Oliger, A., Simpas, J. B. and Gao, H. (2003). OH and HO_2 Chemistry in the urban atmosphere of New York City. *Atmos. Environ., 37*(26), 3639-3651. doi:https://doi.org/10.1016/S1352-2310(03)00459

Rodgers, M. O. and Davis, D. D. (1989). A UV-photofragmentation/laser-induced fluorescence sensor for the atmospheric detection of HONO. *Environ. Sci. Technol., 23*(9), 1106-1112.

Schiller, C. L., Locquiao, S., Johnson, T. J. and Harris, G. W. (2001). Atmospheric Measurements of HONO by Tunable Diode Laser Absorption Spectroscopy. *J. Atmos. Chem., 40*(3), 275-293. doi:10.1023/a:1012264601306

Sofen, E. D., Alexander, B., Steig, E. J., Thiemens, M. H., Kunasek, S. A., Amos, H. M. and Saltzman, E. S. (2014). WAIS Divide ice core suggests sustained changes in the atmospheric formation pathways of sulfate and nitrate since the 19th century in the extratropical Southern Hemisphere. *Atmos. Chem. Phys., 14*(11), 5749-5769. doi:10.5194/acp-14-5749-2014

Solomon, S. (1999). Stratospheric ozone depletion: A review of concepts and history. *Rev. of Geophys., 37*(3), 275-316. doi:10.1029/1999RG900008

Spataro, F. and Ianniello, A. (2014). Sources of atmospheric nitrous acid: State of the science, current research needs, and future prospects. *J. AirWaste Manag. Assoc.*, *64*(11), 1232-1250. doi:10.1080/10962247.2014.952846

Stockwell, W. R. and Calvert, J. G. (1978). The near ultraviolet absorption spectrum of gaseous HONO and N_2O_3. *J. Photochem.*, *8*(2), 193-203. doi:https://doi.org/10.1016/0047-2670(78)80019-7

Stutz, J., Kim, E. S., Platt, U., Bruno, P., Perrino, C. and Febo, A. (2000). UV-visible absorption cross sections of nitrous acid. *J. Geophys. Res.-Atmos.*, *105*(D11), 14585-14592. doi:10.1029/2000JD900003

Takenaka, N., Terada, H., Oro, Y., Hiroi, M., Yoshikawa, H., Okitsu, K. and Bandow, H. (2004). A new method for the measurement of trace amounts of HONO in the atmosphere using an air-dragged aqua-membrane-type denuder and fluorescence detection. *Analyst, 129*(11), 1130-1136. doi:10.1039/b407726a

Thiemens, M. H. (2001). The Mass-Independent Ozone Isotope Effect. *Science, 293*(5528), 226-226. doi:10.1126/science.1063648

Thiemens, M. H. (2006). History and applications of mass-independent isotope effects. *Annual Review of Earth and Planetary Sciences, 34*(1), 217-262. doi:10.1146/annurev.earth.34.031405.125026

Vecera, Z. and Dasgupta, P. K. (1991). Measurement of atmospheric nitric and nitrous acids with a wet effluent diffusion denuder and low-pressure ion chromatography-postcolumn reaction detection. *Anal. Chem.*, *63*(20), 2210-2216. doi:10.1021/ac00020a003

Walters, W. W., Tharp, B. D., Fang, H., Kozak, B. J. and Michalski, G. (2015). Nitrogen Isotope Composition of Thermally Produced NOx from Various Fossil-Fuel Combustion Sources. *Environ. Sci. Technol.*, *49*(19), 11363-11371. doi:10.1021/acs.est.5b02769

Zatko, M., Geng, L., Alexander, B., Sofen, E. and Klein, K. (2016). The impact of snow nitrate photolysis on boundary layer chemistry and the recycling and redistribution of reactive nitrogen across Antarctica and Greenland in a global chemical transport model. *Atmos. Chem. Phys.*, *16*(5), 2819-2842. doi:10.5194/acp-16-2819-2016

Zatko, M. C., Grenfell, T. C., Alexander, B., Doherty, S. J., Thomas, J. L. and Yang, X. (2013). The influence of snow grain size and impurities on the vertical profiles of actinic flux and associated NOx emissions on the Antarctic and Greenland ice sheets. *Atmos. Chem. Phys.*, *13*(7), 3547-3567. doi:10.5194/acp-13-3547-2013

Zhou, X., Qiao, H., Deng, G. and Civerolo, K. (1999). A Method for the Measurement of Atmospheric HONO Based on DNPH Derivatization and HPLC Analysis. *Environ. Sci. Technol.*, *33*(20), 3672-3679. doi:10.1021/es981304c

Nitrogen oxides dictionary (2008), Maruzen. *in Japanese.*

Chapter 2: Spatial Variation of Isotopic Compositions of Snowpack Nitrate Related to Post-depositional Processes in Eastern Dronning Maud Land, East Antarctica

2.1 Introduction

Nitrate (HNO_3(g) + p-NO_3^-) is one of the final oxidation products of reactive nitrogen species (NO_y: NO, NO_2 and HONO) in the atmosphere; it is also one of the major ions found in polar ice cores. Therefore, nitrate in ice cores is a potential proxy for NO_y levels in the atmosphere of the past (Dibb *et al.*, 1998). Solar variability on centennial to millennial time scales may imprint on the long-term NO_3^- record, as suggested by Traversi *et al.* (2012) in their work on the Talos Dome core record. However, a hypothesis linking NO_3^- spikes to Solar Energetic Particle (SEP) events has recently been discredited (Duderstadt *et al.*, 2016; Wolff *et al.*, 2012, 2016). A fundamental difficulty in interpreting the concentration of nitrate in ice cores is that nitrate is not stable after deposition to the snow surface, especially at sites with low snow accumulation (Blunier *et al.*, 2005; Frey *et al.*, 2009), which leads to net loss and redistribution within the snowpack (Frey *et al.*, 2009; Jacobi and Hilker, 2007; Röthlisberger *et al.*, 2000). The relative importance of post-depositional loss processes, *i.e.* volatilization of nitric acid (HNO_3) and photolysis of nitrate, has long been debated (Blunier *et al.*, 2005; Röthlisberger *et al.*, 2000). However, using the stable isotopic composition of nitrate in snow, it has recently been shown in field, laboratory and model experiments that nitrate loss driven by UV photolysis dominates, especially under cold conditions (Berhanu *et al.*, 2014; Erbland *et al.*, 2013; Frey *et al.*, 2009). HNO_3 volatilization and associated isotopic fractionation may become important at warmer temperatures, greater than −20°C (Erbland *et al.*, 2013). To date, attention has focused on the spatial variability of photolytic NO_3^- loss from

surface snow in East Antarctica. This variability has been investigated along a traverse between the Dumont d'Urville station (in Adelie Land) and Vostok, passing through Dome C (Erbland *et al.*, 2013), as well as along one from the East Antarctic coast to Dome Argus (Shi *et al.*, 2015). Based on these studies, it is apparent that, at low accumulation sites, nitrate photolysis results in decreased nitrate concentration in the surface snow, from hundreds to tens of μg L^{-1} below a depth of 10 cm, and with $\delta^{15}N(NO_3^-)$ values correspondingly increased. Spatial variation in NO_3^- concentrations and nitrate isotopic compositions ($\delta^{15}N(NO_3^-)$, $\delta^{18}O(NO_3^-)$ and $\Delta^{17}O(NO_3^-)$) in snowpack along a latitudinal transect between Syowa and Dome Fuji station have not previously been investigated. This study investigates such spatial variation in eastern Dronning Maud Land, East Antarctica, for comparison with results from other traverses.

2.2 Materials and Methods

2.2.1 Sampling Sites

Snow samples were collected in eastern Dronning Maud Land, during the 54th and 57th Japanese Antarctic Research Expedition (JARE). On JARE54, surface snow samples were collected along a coastal–inland traverse, between 25 November 2012 and 13 January 2013 (Fig. 1). Samples were collected and measured throughout the entire depth of between 0 to 30, 50, or 80 cm, as summarized in Table 1 Prior to nitrate measurements, the same melted snow samples were used for sulfur isotopic measurements (Uemura *et al.*, 2016) and subsequently stored for about six months at 4° C, until nitrate was measured. Coastal snow samples were collected during JARE57 at six sites (S30, H42, H68, H80, H108 and H128), between 30 January 2016 and 5 February 2016 (Fig. 1). These were stored at −20 °C until the nitrate measurements – from the surface to a depth of 50 cm – were made.

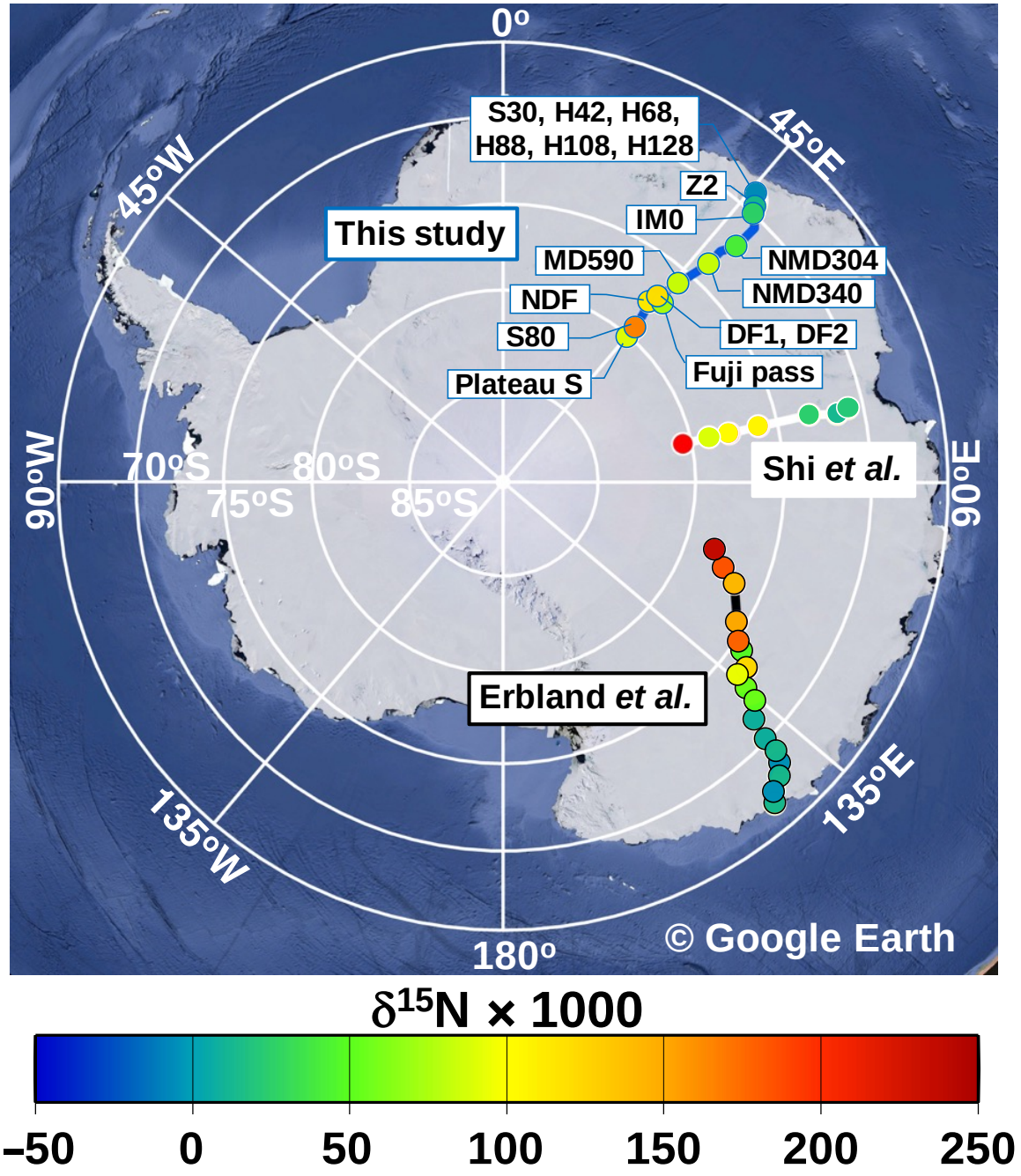

Fig. 1 Spatial distribution of $\delta^{15}N(NO_3^-)$ in surface snow. Snow sampling sites are along traverses from Syowa to Dome Fuji, from French Dumont d'Urville station to Vostok, and from the East Antarctic coast to Dome A. The map was generated using Google Earth (https://www.google.co.jp/intl/ja/earth/).

2.2.2 Chemical and Isotopic Analyses

The concentrations of SO_4^{2-}, Cl^-, NO_3^-, $CH_3SO_3^-$, Na^+, Ca^{2+}, Mg^{2+}, K^+, and NH_4^+ were measured using an ion chromatograph (Dionex ICS-5000+; Thermo Fisher Scientific, Waltham, MA, USA) at the National Institute of Polar Research. To carry out stable isotope analyses, the NO_3^- in ice samples was separated from other ions using ion chromatography. In our setup, the outflow was collected by a fraction collector (CHF122SC; Advantec MFS, Inc., Dublin, CA, USA), as described in our previous study of coastal Antarctic aerosols (Ishino *et al.*, 2017). The sample was pumped at a flow rate of ~1 mL min^{-1} to a pre-concentration column (IonPac AG15, 4 × 50 mm; Dionex Corp., Sunnyvale, CA, USA). Once the sample was loaded onto the concentration column, anions were eluted using a KOH eluent under a gradient mode. Anions were passed through a guard column (IonPac AG19, 4 × 50 mm; Dionex Corp.) and a separation column (IonPac AS19, 4 × 250 mm, Dionex Corp.). In order to test for possible changes in isotopic compositions of NO_3^- during ion chromatographic (IC) separation, we compared results – with or without IC separation – of reference materials USGS 32, 34 and 35, prepared in 18.2 MΩ cm water (Table 2). The differences between with and without IC separation were slightly correlated with isotopic compositions. Sample measurements were therefore also calibrated by using the correlation slope, for measuring $\delta^{15}N(NO_3^-)$, $\delta^{18}O(NO_3^-)$ and $\Delta^{17}O(NO_3^-)$, in order to avoid bias.

Table 1 Sample location, sampling date, altitude, latitude, longitude, depth, [NO_3^-], $\delta^{15}N$, $\delta^{18}O$, $\Delta^{17}O$, and traverse information for sites mentioned in this study. DF 1 and 2 denote the Dome Fuji station, where a deep ice core was drilled (Dome Fuji Ice Core Project Members, 2017).

Location	Sampling date	altitude	Latitude	Longitude	Depth	[NO_3^-]	$\delta^{15}N$	$\delta^{18}O$	$\Delta^{17}O$	Traverse
	D. M. Y	(m, a.s.l.)	(°S)	(°E)	(cm)	(μg L^{-1})		(‰)		
Z2	25 Nov 2012	1924	70.0	42.4	0−80	52.3	20.6	69.1	27.4	JARE54
IM0	27 Nov 2012	2215	70.7	44.3	0−50	102.5	25.7	66.1	26.9	JARE54
NMD196	3 Dec 2012	2845	72.2	44.3	0−50	79.8	*N.D.*	*N.D.*	*N.D.*	JARE54
NMD304	5 Dec 2012	3192	73.1	42.9	0−50	69.5	41.1	55.4	24.1	JARE54
NMD370	8 Dec 2012	3338	74.1	43.0	0−50	83.1	*N.D.*	*N.D.*	*N.D.*	JARE54
MD590	12 Dec 2012	3684	76.0	41.1	0−50	104.1	83.5	68.8	31.9	JARE54
DF1	20 Dec 2012	3803	77.3	39.7	0−30	94.0	127.3	51.3	29.4	JARE54
NDF	25 Dec 2012	3763	77.8	39.1	0−30	71.2	111.7	44.0	24.9	JARE54
Plateau S	28 Dec 2012	3678	79.4	40.5	0−30	80.3	165.5	37.5	24.5	JARE54
S80	2 Jan 2013	3625	80.0	40.5	0−30	130.8	90.7	37.7	20.3	JARE54
Fuji pass	8 Jan 2013	3787	77.4	41.5	0−30	92.4	74.3	19.8	13.2	JARE54
DF2	13 Jan 2013	3803	77.3	39.7	0−30	79.8	118.6	25.0	18.7	JARE54
S30	3 Feb 2016	986	69.0	40.7	0−50	40.0	-19.0	75.8	28.2	JARE57
H42	3 Feb 2016	1101	69.1	40.9	0−50	65.4	-6.6	85.5	30.8	JARE57
H68	3 Feb 2016	1164	69.2	41.1	0−50	66.5	-14.5	82.3	28.8	JARE57
H88	3 Feb 2016	1244	69.3	41.2	0−50	124.3	-19.4	83.7	30.3	JARE57
H108	3 Feb 2016	1315	69.3	41.4	0−50	87.9	-6.4	77.8	30.0	JARE57
H128	30 Jan 2016	1376	69.4	41.6	0−50	38.5	14.1	91.0	34.5	JARE57

N.D.: not determined

Isotopic compositions of NO_3^- in solution were measured using a bacterial method, coupled with N_2O decomposition via microwave-induced plasma (MIP) (Hattori *et al.*, 2016). Briefly, 100 nmol NO_3^- was converted to N_2O by a strain of denitrifying bacteria, having no N_2O reductase. The N_2O produced was then isolated using chemical

traps and gas chromatography; it was decomposed to O_2 and N_2 using MIP. The isotopic compositions of O_2 and N_2 were measured using isotope-ratio mass spectrometry (MAT253; Thermo Fisher Scientific). Isotopic reference materials, as well as USGS 32, 34, 35, and their mixtures, prepared in 18.2 MΩ cm water, were also analyzed using the same analytical process as our samples, for normalization. Stable isotopic compositions are reported as: $\delta X = R_{sample}/R_{reference} - 1$, where X denotes ^{15}N, ^{17}O, or ^{18}O, and R denotes the isotope ratios $^{15}N/^{14}N$, $^{17}O/^{16}O$, and $^{18}O/^{16}O$, determined for both sample and standard materials. The δ values are reported as per mil (‰). The $\delta^{15}N$ value is relative to atmospheric N_2 (air), whereas $\delta^{18}O$ and $\delta^{17}O$ values are relative to Vienna Standard Mean Ocean Water (VSMOW). $\Delta^{17}O$ notation is used in this study to identify mass-independent fractionation of oxygen, which causes deviation from a mass-dependent fractionation line. $\Delta^{17}O$ is defined here by the linear approximation $\Delta^{17}O = \delta^{17}O - 0.52 \times \delta^{18}O$. By propagating analytical uncertainties for the IC separation and replicate isotopic measurements of USGS 34, 35 and 32, the estimated combined uncertainties were 0.6 ‰, 1.8 ‰, and 0.3 ‰ for $\delta^{15}N(NO_3^-)$, $\delta^{18}O(NO_3^-)$ and $\Delta^{17}O(NO_3^-)$, respectively.

2.3 Results

Figure 2 shows altitude, snow accumulation rate (*A*), NO_3^- concentrations, and $\delta^{15}N(NO_3^-)$ values for each sampling site plotted against latitude. Values for *A* decrease with increasing elevation, from coastal to inland sites (Figs 2a and 2b; data are from (Hoshina *et al.*, 2016). NO_3^- concentrations in surface snow from coastal to inland sites ranged from 38.5 to 130.8 μg L^{-1}, without any specific trend with latitude (Fig. 2c). A wide variation in $[NO_3^-]$ in surface snow at coastal sites was observed during JARE57, having values from 38.5 to 124.3 μg L^{-1} (Table 1). In contrast, a narrow range in $[NO_3^-]$ was observed at inland sites on JARE54, having values from 71.2 to 130.8 μg L^{-1} (Table 1). Along a previous traverse between Syowa to Dome Fuji (Suzuki *et al.*, 2003), NO_3^- concentrations at inland sites were 430 ± 100 μg L^{-1}, approximately four times higher than those observed in this study. This difference can be explained by the different sampling depth of Suzuki *et al.* (2003) (surface ~ 3 cm) compared with this study (0–30 cm). As explained below, our $\delta^{15}N(NO_3^-)$ results indicate that NO_3^- concentrations were influenced by post-depositional loss. The $\delta^{15}N(NO_3^-)$ in surface snow clearly increases from −19.4 to 165.5 ‰ along this transect, moving from low- to high-latitudes (Fig. 1 and 2d). The $\delta^{15}N(NO_3^-)$ values observed in costal surface snow on JARE57 and JARE54 were −19.4 to −6.4 ‰ and 20.6 to 25.7 ‰, respectively. Meanwhile, the $\delta^{15}N$ values observed in inland surface snow on JARE54 were 41.0 to 165.5 ‰.

Table 2 Comparison of isotope measurements of USGS 34, USGS 35 and USGS 32, with and without ion chromatographic (IC) separation.

Sample	With IC separation					Without IC separation				
	n	$\delta^{15}N$	$\delta^{17}O$	$\delta^{18}O$	$\Delta^{17}O$	n	$\delta^{15}N$	$\delta^{17}O$	$\delta^{18}O$	$\Delta^{17}O$
		(‰)					(‰)			
USGS34	2	−1.4 ± 0.10	−13.0 ± 0.2	−25.4 ± 0.3	0.2 ± 0.0	12	−1.8 ± 0.10	−14.5 ± 0.3	−27.7 ± 0.3	0.0 ± 0.1
USGS35	2	2.7 ± 0.04	51.1 ± 0.2	57.0 ± 1.2	21.5 ± 0.4	12	2.7 ± 0.1	51.7 ± 0.5	57.7 ± 0.6	21.7 ± 0.2
USGS32	2	179.1 ± 0.06	13.4 ± 0.1	25.8 ± 0.6	0.0 ± 0.4	8	180.0 ± 0.2	12.4 ± 0.4	24.8 ± 0.9	−0.4 ± 0.1

n: number of measurements, uncertainties: one-σ

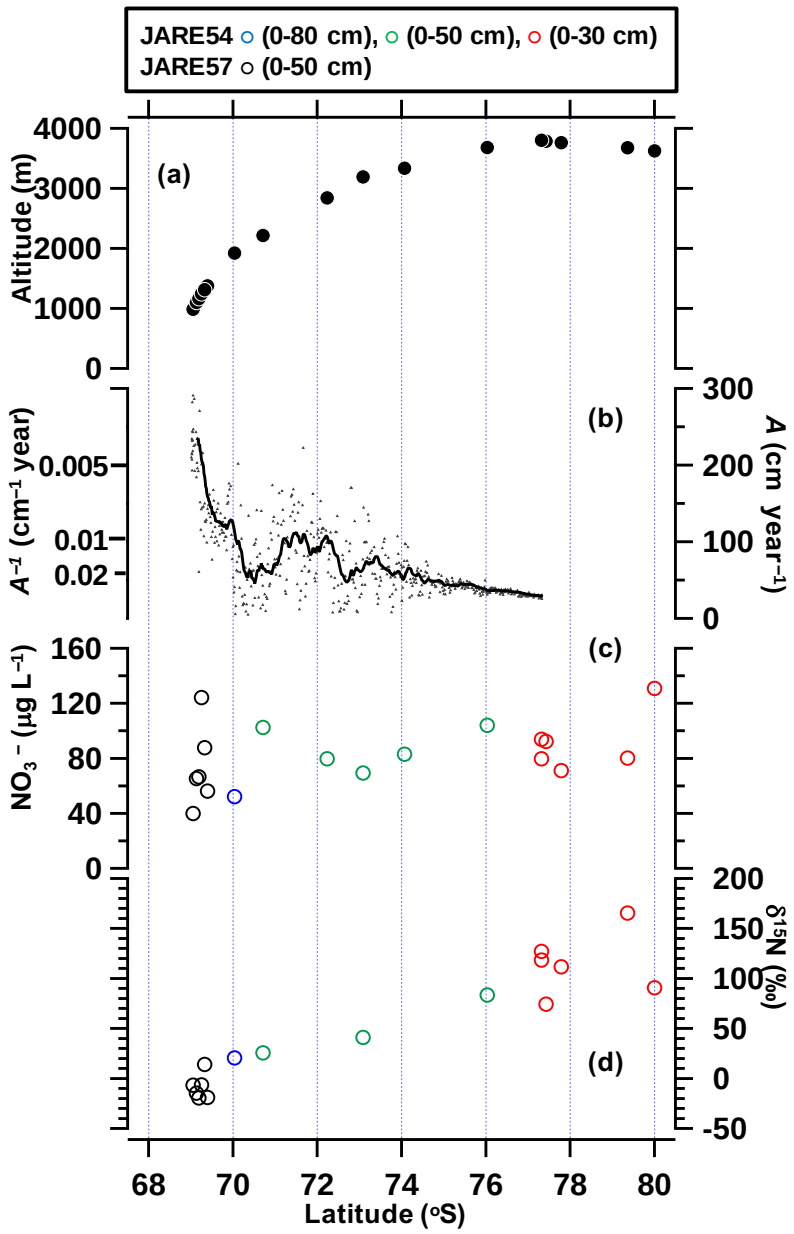

Fig. 2 Altitude (a), snow accumulation rate (Hoshina et al., 2016) (b), nitrate concentration (c), and nitrogen isotopic composition of nitrate (d) as a function of latitude within East Antarctica. For (c) and (d), colors of plots represent the sampling depth and Traverse (Black: JARE57 (0–50 cm), Blue: JARE54 (0–80 cm), Green: JARE54 (0–50 cm) and Red: JARE54 (0–30 cm)).

2.4 Discussion

2.4.1 Spatial Variation of Nitrate and Its Isotopic Composition in East Antarctica

To explain the increasing trend in $\delta^{15}N(NO_3^-)$ values (Fig. 2d) with elevation, it is necessary to consider nitrogen source, post-depositional loss (through photolysis and sublimation) and redistribution of re-emitted NO_y. Atmospheric measurements on the Antarctic coast at Halley show that organic NO_y (CH_3NO_3 and PAN) dominate in winter and are consistent with an oceanic source (Jones *et al.*, 2011). However, surface snow nitrate strongly correlates with inorganic NO_y (especially HNO_3) (Jones *et al.*, 2011), indicating that the snow nitrate is dominated by HNO_3. Degradation products of organic nitrate can form nitrate only indirectly, via NO_x production (e.g., see introduction in Savarino *et al.*, 2007). Further inland, on the high Plateau, the influence of tropospheric sources would become less important, especially in winter, and the stratospheric inputs dominate, as supported by isotope measurements (Savarino *et al.*, 2007; Wagenbach *et al.*, 1998). Therefore, the main source of nitrate is from UV destruction of nitrous oxide (N_2O) in the stratosphere. In this study the initial $\delta^{15}N(NO_3^-)$ was calculated as $\delta^{15}N$ (particle NO_3^-) $\approx \delta^{15}N(HNO_3) \approx \delta^{15}N(NO) = 19 \pm 3$ ‰ (Savarino *et al.*, 2007). Once deposited, this nitrate is influenced by UV photolysis, whereby the $^{14}NO_3^-$ isotopologue is removed faster than the $^{15}NO_3^-$ isotopologue (Berhanu *et al.*, 2014), leading to enrichment of $\delta^{15}N(NO_3^-)$ in the remaining nitrate. On the inland Antarctic plateau, we assume that a single and irreversible process of NO_3^- loss occurs, because the physical release such as volatilization of nitrate leads to only a minor net mass loss (Erbland *et al.*,

2013).

To quantify the effect of nitrate loss related to photolysis, the $^{15}N/^{14}N$ fractionation factor ($^{15}\varepsilon$) is expressed, based on a Rayleigh model, as follows: $\ln(\delta^{15}N_R + 1) = {}^{15}\varepsilon \ln f + \ln(\delta^{15}N_0 + 1)$, where $\delta^{15}N_0$ and $\delta^{15}N_R$ denote δ values for initial and remaining NO_3^-, respectively; and f is the remaining mass fraction of NO_3^- (Blunier *et al.*, 2005). The remaining NO_3^- mass fraction f can be evaluated using measured $\delta^{15}N(NO_3^-)$ values from this study, assuming an initial $\delta^{15}N_0$ value of 19 ± 3‰; (Savarino *et al.*, 2007), and an $^{15}\varepsilon$ for UV photolysis of nitrate, based on laboratory experiments simulated for the Dome C site (−47.9 ± 6.8 ‰, (Berhanu *et al.*, 2014)). Thus, the remaining nitrate mass fraction was calculated to be 11 ± 5, 15 ± 6, 5 ± 3, 23 ± 8, 32 ± 9, and 13 ± 5 % for sites DF1, NDF, Plateau S, S80, Fuji Pass, and DF2, respectively. These values are based on stratospheric input only. If tropospheric sources are also significant, the results will need to be revised accordingly.

In contrast, it is oversimplifying to apply only an $^{15}\varepsilon$ related to photolysis of NO_3^-, when calculating f at coastal sites in Antarctica. This is because sublimation and redistribution of recycled NO_y affect both NO_3^- concentrations and $\delta^{15}N(NO_3^-)$. In fact, the $\delta^{15}N(NO_3^-)$ values at coastal sites (S30, H42, H68, H80, H108 and H128) ranged from −18.7 to 14.2 ‰ (Table 1 and Fig. 2d); these values were lower than $\delta^{15}N(NO_3^-)$ values of nitrate from the stratosphere (19 ± 3 ‰; (Savarino *et al.*, 2007)). This suggests that other factors influence the $\delta^{15}N(NO_3^-)$ deposited at coastal sites. These lower $\delta^{15}N(NO_3^-)$ values can be explained by nitrogen dynamics and the redistribution of nitrate occurring

in Antarctica. For example, the $\delta^{15}N(NO_3^-)$ values of atmospheric nitrate in spring in Antarctica are comparatively low ($\delta^{15}N$: −32.7 ± 8.4 ‰) (Savarino *et al.*, 2007). Such re-emitted NO_y inland transported to coastal sites via katabatic winds would result in lower $\delta^{15}N(NO_3^-)$ values observed in coastal snow. Furthermore, nitrate concentrations observed in the coastal surface snow samples from S30, H42, H68, H88, H108 and H128 along the JARE57 traverse showed a 3-fold variation (Fig. 2c). The $\delta^{15}N(NO_3^-)$ from surface snow at sites S30 to H108 exhibited relatively small variation, ranging from −18.7 to −6.2 ‰, while the $\delta^{15}N(NO_3^-)$ value at H128 was higher (14.2 ‰) than for other samples (Fig. 2d; Table 1). Given that $\delta^{15}N(NO_3^-)$ values in the coastal snow are lower than in nitrate from the stratosphere, the low values of $\delta^{15}N(NO_3^-)$ are likely related to the redistribution of nitrate. Thus, the main process determining NO_3^- concentrations in the coastal area is probably the redistribution (*i.e.*, (i) vertical redistribution of NO_3^- within the snowpack driven by nitrate photolysis; (ii) horizontal redistribution via advective transport of emissions (NO_y and HNO_3) and re-deposition further downwind or in near-coastal areas (Savarino *et al.*, 2007; Frey *et al.*, 2009)) of re-oxidized NO_y, emitted via photolysis of nitrate in the snowpack, further inland. This explains the inhomogeneity in nitrate concentrations on the surface snow at the coastal sites.

2.4.2 Comparison with Other Sites in East Antarctica

Figure 3a shows relationships among $\delta^{15}N(NO_3^-)$ and *A* values along three different traverses: from Syowa station to Dome Fuji station (this study), from Dumont d'Urville station to Vostok, passing through Dome C (Erbland *et al.*, 2013), as well as

from the East Antarctic coast to Dome A (Shi *et al.*, 2015). The *A* values for Fuji pass, NDF, Plateau S, and S80 were not directly estimated in this study; they were estimated based on an extrapolation of a linear regression between *A* and altitude. The data from Shi et *al.* (2015) were compared as concentration-weighted averages for the same sample depth with our samples. Because sampling depths at the coastal sites of Erbland *et al.* (2013) were not the same as our samples (i.e., they were shallower than 30 cm), a weighted average of all samples measured in their study was calculated (Fig. 3). Given that the contribution of nitrate photolysis is considered to be minor at coastal sites (Savarino *et al.*, 2007), the difference in value related to this sampling depth difference is likely to be small. Overall, the trends in $\delta^{15}N(NO_3^-)$ values and *A* were similar among all three traverses, yielding a regression line with a slope and intercept of 4146.2 ± 279.7 and 15.1 ± 7.4 (R^2 = 0.84), respectively (Fig. 3a). We conclude that spatial variation in $\delta^{15}N(NO_3^-)$ is caused by different contributions of UV photolyzed nitrate to the snowpack. This redistribution of nitrate can be characterized as a function of *A* throughout East Antarctica.

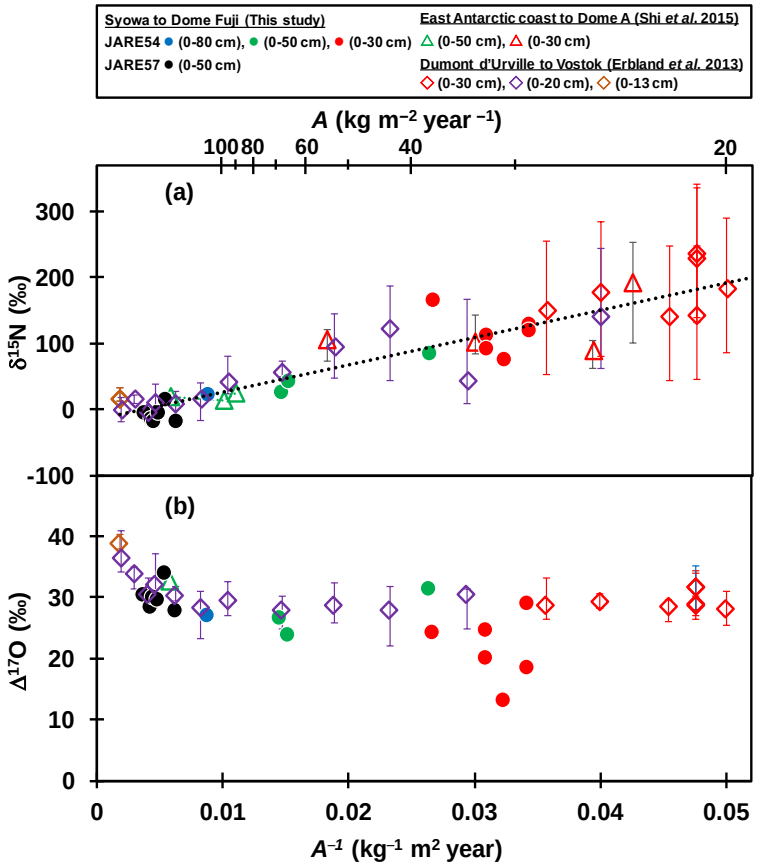

Fig. 3. Values for $\delta^{15}N$ (a) and $\Delta^{17}O$ (b) from nitrate in surface snow as a function of the inverse of the snow accumulation rate A^{-1} (bottom horizontal axis) and the snow accumulation rate A (top horizontal axis). Error bars indicate maximum and minimum values at each pit. A dotted black line in (a) indicates the linear regression line $\delta^{15}N = 4146.2 \times A^{-1} - 15.1$. The $\delta^{15}N$ and $\Delta^{17}O$ for Shi et al. (2015) and Erbland et al. (2013) were recalculated by concentration-weighted averages for matching the core depths of this study. Circles: Syowa to Dome Fuji (JARE54 and 57, This study); Triangles: East Antarctic coast to Dome C (Shi et al., 2015) (0-50 cm and 0-30 cm, respectively); Diamonds: Dumont d'Urville to Vostok (Erbland et al., 2013) (0-30 cm, 0-20 cm and 0-13 cm, respectively).

The relationship between $\Delta^{17}O$ values of nitrate and *A* along the two JARE traverses (JARE54 and 57; this study), as well as the Erbland *et al.* (2013) traverse and a snow pit from the Shi *et al.*, (2015) traverse are shown in Fig. 3b. The $\Delta^{17}O$ values of nitrate collected on JARE57 (S30, H42, H68, H88, H108 and H128) ranged from 27.8‰ to 34.0‰ (Table 1), which is in good agreement with coastal sites data from Erbland *et al.* (2013) and Shi *et al.* (2015) (Fig. 3b). Results from the samples collected on JARE54 were also generally consistent with those from previous traverses (Fig. 3b). However, values for three samples (S80, Fuji pass, and DF2) ranged from 13.2 to 20.3 ‰, i.e. lower than for JARE54 and earlier traverses. The sampling dates of DF1 and DF2 differed by several days, whereas the places are only a few meters from each other. In addition, the NO_3^- concentration and $\delta^{15}N(NO_3^-)$ values of samples DF1 and DF2 were similar. Interestingly, there was a large difference of $\Delta^{17}O(NO_3^-)$ between DF1 and DF2. Low $\Delta^{17}O(NO_3^-)$ values of nitrate in the surface snow cannot be explained by the $\Delta^{17}O(NO_3^-)$ values of atmospheric nitrate, which has a summer minimum (~ 20‰; Savarino *et al.*, 2007). It also is unlikely that analytical errors caused these low $\Delta^{17}O(NO_3^-)$ values, because the measurements of standards and blank were normal. Isotopic exchange between the sample's nitrate and water at some stage during storage or analysis has also been excluded, given that the half-life for oxygen isotope exchange under natural conditions (25°C, pH 7) is estimated to be around 5.5×10^9 years (Kaneko and Poulson, 2013). Thus, it is difficult to explain these low $\Delta^{17}O(NO_3^-)$ values in S80, Fuji pass, and DF2 samples from JARE54. Similarly unexpected low oxygen isotopic compositions ($\delta^{18}O(NO_3^-)$ values for that study) were also reported in ice cores drilled at

Lomonosovfonna, Svalbard (Vega *et al.*, 2015). Future study is clearly needed to test the spatial extent and variation of these unexpectedly low oxygen isotope values in snow at inland sites. Perhaps they are related to the spatio-temporal distribution of snow. Except for the low values of $\Delta^{17}O(NO_3^-)$ in nitrate from these three samples, the $\Delta^{17}O(NO_3^-)$ values of nitrate and its relationship to *A* between Syowa and Dome Fuji were generally consistent with other traverses.

2.4.3 Implications for the Use of Nitrate as an Ice Core Proxy

Nitrate concentrations in the Talos Dome ice core were proposed as a solar activity proxy for the Holocene. Such interpretation is supported by insignificant loss of nitrate in snow pit material at the Talos Dome site (Traversi *et al.*, 2012). Based on the linear regression between A^{-1} and $\delta^{15}N(NO_3^-)$ values derived in this study (Fig. 3a), for a snow accumulation rate of ca. 72 kg m^{-2} $year^{-1}$ at Talos Dome, the $\delta^{15}N(NO_3^-)$ value at Talos Dome is estimated to be 56.5 ± 8.6 ‰. This is higher than for nitrate derived from the stratosphere (19 ± 3‰; Savarino *et al.*, 2007), suggesting that the Talos Dome site must be influenced by UV photolysis. Whatever the case, reconstruction of past solar activity using nitrate concentrations in ice cores requires careful consideration given that vertical and/or horizontal redistribution of nitrate is occurring in this region.

In addition to $\delta^{15}N(NO_3^-)$ values, it is worth mentioning the possible application of oxygen isotopic compositions of nitrate for the Antarctic samples. Whereas atmospheric nitrate inherits a large positive oxygen isotopic anomaly (^{17}O excess) from ozone, other oxidants such as OH possess lower $\Delta^{17}O$ values. In particular, seasonal

variation of $\Delta^{17}O$ values of sulfate and nitrate in coastal Antarctica suggest that $\Delta^{17}O$ values were controlled by oxidant species and not by seasonal changes in $\Delta^{17}O$ values of O_3 (Ishino et al., 2017). Thus, the $\Delta^{17}O$ of nitrate in Antarctic ice cores has the potential to reconstruct historical changes in relative abundance of atmospheric O_3 and HO_x over long time periods, based on the WAIS Divide ice core (Sofen *et al.*, 2014). However, similar to nitrogen, oxygen isotopic compositions of nitrate are also changed by post depositional processes, especially at sites which have low accumulations of snow. Recently, a chemical model of nitrate behavior at the air–snow interface on the East Antarctic Plateau has been developed, to reconstruct $\Delta^{17}O(NO_3^-)$ values in the atmosphere. Our new traverse data (Fig. 3b) will provide additional constraints to parameters used in such a chemical model. In turn, this will help establish the mechanisms contributing to the low $\Delta^{17}O(NO_3^-)$ values in inland areas. The determination of past atmospheric $\Delta^{17}O(NO_3^-)$ values from ice core analysis (Erbland *et al.*, 2015), coupled with global atmospheric chemical transport model such as GEOS-Chem, which quantify atmospheric nitrate formation pathways (Alexander *et al.*, 2009), provides the scope for reconstructing past atmospheric oxidizing capacity and its relationship to past global changes.

2.5 Conclusion

We report spatial variations in NO_3^- isotopic compositions from coastal to inland sites in eastern Dronning Maud Land, East Antarctica. Although the NO_3^- concentrations

of surface snow between coastal and inland sites ranged from 40.0 to 130.8 μg L^{-1}, without explicit trends with latitude, the $\delta^{15}N(NO_3^-)$ values in the surface snow increased along the traverse from coastal to inland sites, ranging from −19.4 to 165.5 ‰. Based on a Rayleigh model, the remaining nitrate mass fraction was calculated to vary from 5% to 32% at sites DF1, NDF, Plateau S, S80, Fuji Pass, and DF2. This suggests that, at these inland sites, between 68 and 95 % of nitrate was removed via UV photolysis of the snowpack. In contrast, the $\delta^{15}N(NO_3^-)$ values at coastal sites were lower than $\delta^{15}N$ values of stratospheric nitrate, exhibiting a large variation in nitrate concentrations but a small variation in $\delta^{15}N(NO_3^-)$ values. This indicates that the horizontal redistribution via advective transport of nitrate has an important effect on nitrate concentrations in surface snow at coastal sites. The relationship between the isotopic values ($\delta^{15}N(NO_3^-)$ and $\Delta^{17}O(NO_3^-)$) and snow accumulation rate is consistent with previous traverses across East Antarctica, implying that UV-driven post-depositional loss and horizontal redistribution occur similarly throughout East Antarctica.

References

Alexander, B., Hastings, M. G., Allman, D. J., Dachs, J., Thornton, J. A. and Kunasek, S. A. (2009). Quantifying atmospheric nitrate formation pathways based on a global model of the oxygen isotopic composition ($\Delta^{17}O$) of atmospheric nitrate. *Atmos. Chem. Phys.*, *9*(14), 5043-5056. doi:10.5194/acp-9-5043-2009

Berhanu, T. A., Meusinger, C., Erbland, J., Jost, R., Bhattacharya, S. K., Johnson, M. S. and Savarino, J. (2014). Laboratory study of nitrate photolysis in Antarctic snow. II. Isotopic effects and wavelength dependence. *J. Chem. Phys.*, *140*(24), 244306. doi:10.1063/1.4882899

Blunier, T., Floch, G. L., Jacobi, H.-W. and Quansah, E. (2005). Isotopic view on nitrate loss in Antarctic surface snow. *Geophys. Res. Lett.*, *32*(13), L13501. doi:10.1029/2005GL023011

Dibb, J. E., Talbot, R. W., Munger, J. W., Jacob, D. J. and Fan, S.-M. (1998). Air-snow exchange of HNO_3 and NO_y at Summit, Greenland. *J. Geophys. Res.-Atmos*, *103*(D3), 3475-3486. doi:10.1029/97JD03132

Duderstadt, K. A., Dibb, J. E., Schwadron, N. A., Spence, H. E., Solomon, S. C., Yudin, V. A., Jackman, C. H. and Randall, C. E. (2016). Nitrate ion spikes in ice cores not suitable as proxies for solar proton events. *J. Geophys. Res.-Atmos, 121*(6), 2994-3016. doi:10.1002/2015JD023805

Erbland, J., Savarino, J., Morin, S., France, J. L., Frey, M. M. and King, M. D. (2015). Air–snow transfer of nitrate on the East Antarctic Plateau – Part 2: An isotopic model for the interpretation of deep ice-core records. *Atmos. Chem. Phys.*, *15*(20),

12079-12113. doi:10.5194/acp-15-12079-2015

Erbland, J., Vicars, W. C., Savarino, J., Morin, S., Frey, M. M., Frosini, D., Vince, E. and Martins, J. M. F. (2013). Air–snow transfer of nitrate on the East Antarctic Plateau – Part 1: Isotopic evidence for a photolytically driven dynamic equilibrium in summer. *Atmos. Chem. Phys.*, *13*(13), 6403-6419. doi:10.5194/acp-13-6403-2013

Frey, M. M., Savarino, J., Morin, S., Erbland, J. and Martins, J. M. F. (2009). Photolysis imprint in the nitrate stable isotope signal in snow and atmosphere of East Antarctica and implications for reactive nitrogen cycling. *Atmos. Chem. Phys.*, *9*(22), 8681-8696. doi:10.5194/acp-9-8681-2009

Hattori, S., Savarino, J., Kamezaki, K., Ishino, S., Dyckmans, J., Fujinawa, T., Caillon, N., Barbero, A., Mukotaka, A., Toyoda, S., Well, R. and Yoshida, N. (2016). Automated system measuring triple oxygen and nitrogen isotope ratios in nitrate using the bacterial method and N_2O decomposition by microwave discharge. *Rapid Commun. Mass Spectrom.*, *30*(24), 2635-2644. doi:10.1002/rcm.7747

Hoshina, Y., Fujita, K., Iizuka, Y. and Motoyama, H. (2016). Inconsistent relationships between major ions and water stable isotopes in Antarctic snow under different accumulation environments. *Polar Sci.*, *10*(1), 1-10. doi:https://doi.org/10.1016/j.polar.2015.12.003

Ishino, S., Hattori, S., Savarino, J., Jourdain, B., Preunkert, S., Legrand, M., Caillon, N., Barbero, A., Kuribayashi, K. and Yoshida, N. (2017). Seasonal variations of triple oxygen isotopic compositions of atmospheric sulfate, nitrate, and ozone at

Dumont d'Urville, coastal Antarctica. *Atmos. Chem. Phys.*, *17*(5), 3713-3727. doi:10.5194/acp-17-3713-2017

Jacobi, H.-W. and Hilker, B. (2007). A mechanism for the photochemical transformation of nitrate in snow. *J. Photoch. Photobio. A*, *185*(2), 371-382. doi:https://doi.org/10.1016/j.jphotochem.2006.06.039

Jones, A. E., Wolff, E. W., Ames, D., Bauguitte, S. J. B., Clemitshaw, K. C., Fleming, Z., Mills, G. P., Saiz-Lopez, A., Salmon, R. A., Sturges, W. T. and Worton, D. R. (2011). The multi-seasonal NO_y budget in coastal Antarctica and its link with surface snow and ice core nitrate: results from the CHABLIS campaign. *Atmos. Chem. Phys.*, *11*(17), 9271-9285. doi:10.5194/acp-11-9271-2011

Kaneko, M. and Poulson, S. R. (2013). The rate of oxygen isotope exchange between nitrate and water. *Geochim. Cosmochim. Acta*, *118*, 148-156. doi:10.1016/j.gca.2013.05.010

Röthlisberger, R., Hutterli, M. A., Sommer, S., Wolff, E. W. and Mulvaney, R. (2000). Factors controlling nitrate in ice cores: Evidence from the Dome C deep ice core. *J. Geophys. Res.-Atmos*, *105*(D16), 20565-20572. doi:10.1029/2000JD900264

Savarino, J., Kaiser, J., Morin, S., Sigman, D. M. and Thiemens, M. H. (2007). Nitrogen and oxygen isotopic constraints on the origin of atmospheric nitrate in coastal Antarctica. *Atmos. Chem. Phys.*, *7*(8), 1925-1945. doi:10.5194/acp-7-1925-2007

Shi, G., Buffen, A. M., Hastings, M. G., Li, C., Ma, H., Li, Y., Sun, B., An, C. and Jiang, S. (2015). Investigation of post-depositional processing of nitrate in East Antarctic snow: isotopic constraints on photolytic loss, re-oxidation, and source

inputs. *Atmos. Chem. Phys., 15*(16), 9435-9453. doi:10.5194/acp-15-9435-2015

Sofen, E., Alexander, B., Steig, E., Thiemens, M., Kunasek, S., Amos, H., Schauer, A., Hastings, M., Bautista, J. and Jackson, T. (2014). WAIS Divide ice core suggests sustained changes in the atmospheric formation pathways of sulfate and nitrate since the 19th century in the extratropical Southern Hemisphere. *Atmos. Chem. Phys., 14*(11), 5749-5769.

Suzuki, T., Iizuka, Y., Furukawa, T., Matsuoka, K., Kamiyama, K. and Watanabe, O. (2003). *Spatial variability of chemical tracers in surface snow along the route from the coast to 1000km inland at east Dronning Maud Land, Antarctica* (14), 48-56.

Traversi, R., Usoskin, I. G., Solanki, S. K., Becagli, S., Frezzotti, M., Severi, M., Stenni, B. and Udisti, R. (2012). Nitrate in Polar Ice: A New Tracer of Solar Variability. *Solar Physics, 280*(1), 237-254. doi:10.1007/s11207-012-0060-3

Uemura, R., Masaka, K., Fukui, K., Iizuka, Y., Hirabayashi, M. and Motoyama, H. (2016). Sulfur isotopic composition of surface snow along a latitudinal transect in East Antarctica. *Geophys. Res. Lett., 43*(11), 5878-5885. doi:10.1002/2016GL069482

Vega, C. P., Pohjola, V. A., Samyn, D., Pettersson, R., Isaksson, E., Björkman, M. P., Martma, T., Marca, A. and Kaiser, J. (2015). First ice core records of NO_3^- stable isotopes from Lomonosovfonna, Svalbard. *J. Geophys. Res.-Atmos, 120*(1), 313-330. doi:10.1002/2013JD020930

Wagenbach, D., Legrand, M., Fischer, H., Pichlmayer, F. and Wolff, E. W. (1998). Atmospheric near-surface nitrate at coastal Antarctic sites. *J. Geophys. Res.-*

Atmos, 103(D9), 11007-11020. doi:10.1029/97JD03364

Wolff, E. W., Bigler, M., Curran, M. A. J., Dibb, J. E., Frey, M. M., Legrand, M. and McConnell, J. R. (2012). The Carrington event not observed in most ice core nitrate records. *Geophys. Res. Lett., 39*(8), L08503. doi:10.1029/2012GL051603

Wolff, E. W., Bigler, M., Curran, M. A. J., Dibb, J. E., Frey, M. M., Legrand, M. and McConnell, J. R. (2016). Comment on “Low time resolution analysis of polar ice cores cannot detect impulsive nitrate events” by D.F. Smart et al. *J. Geophys. Res.-Spac. Phys., 121*(3), 1920-1924. doi:10.1002/2015JA021570

Chapter 3: NO_y Flux from Snow Surface and the Depth Profile of HONO in Snowpack in Eastern Dronning Maud Land, East Antarctica

3.1 Introduction

Nitrate in snow is subject to post-depositional processing, especially in low-accumulation regions, which leads to net loss and redistribution within the snowpack (Frey *et al.*, 2009; Jacobi & Hilker, 2007; Röthlisberger *et al.*, 2000). The relative importance of post-depositional loss processes, *i.e.* volatilization of nitric acid (HNO_3) and photolysis of nitrate, has long been debated (Blunier *et al.*, 2005; Röthlisberger *et al.*, 2000). Reactive nitrogen oxides (NO_y: NO, NO_2 and HONO) emission to clean atmosphere in Antarctica from snowpack has been observed (Beine *et al.*, 2006; Legrand *et al.*, 2014; Liao *et al.*, 2006). Nitrate photolysis in/on snowpack has been known as a source of NO_y (Honrath *et al.*, 1999; Jones *et al.*, 2001). While the photochemistry of nitrate in the snowpack has significant implications since its photoproducts, NO and NO_2, are intimately linked to reactions involving ozone, hydrocarbons and halogens. This process also generates OH radicals which can oxidize organic matter within snowpack, leading to the formation of oxidized hydrocarbons (*e.g.* formaldehyde, acetaldehyde, acetone) (Domine & Shepson, 2002; Grannas *et al.*, 2006; Sumner & Shepson, 1999). HONO has been measured in the polar regions (Amoroso *et al.*, 2006; Clemitshaw, 2006; Honrath *et al.*, 2002; Zhou *et al.*, 2001), where it has also been suggested as a possible byproduct of nitrate photolysis (Zhou *et al.*, 2001). However, actual HONO concentrations and its source at polar sites have been debated (Jacobi & Hilker, 2007; Kleffmann & Wiessen, 2008; Liao *et al.*, 2006).

Nitrate photolysis in snowpack is a rare source of NO_y for Antarctic clean air. Nitrate undergoes photolysis in quasi liquid layer of ice, then NO_2 (Eq. 1) or NO_2^- (Eq.

2) is produced (Grannas *et al*., 2006; Mack & Bolton, 1999; Meusinger *et al*., 2014).

$NO_3^- + h\nu + H^+ \rightarrow NO_2(aq) + OH(aq)$ (R1)

$NO_3^- + h\nu \rightarrow NO_2^- + O(^3P)(aq)$ (R2)

NO_2 produced in the solution phase evaporates as NO_2 gas (Boxe *et al.*, 2005). Furthermore, NO (Eq. 3), NO_2 (Eq. 4), and HONO (Eq. 5) are produced from NO_2^-.

$NO_2^- + h\nu + H^+ \rightarrow NO(aq) + OH(aq)$ (R3)

$NO_2^- + OH\,(aq) \rightarrow NO_2(aq) + OH^-$ (R4)

$NO_2^- + H^+ \rightarrow HONO(aq)$ (R5)

Through these reactions, NO_y is released into the atmosphere and affects the atmospheric chemistry of Antarctica. There is also a process of HONO generation and nitrate regeneration from NO_2 (Eq. 6).

$2NO_2 + H_2O \rightarrow HONO + HNO_3$ (R6)

Note that HONO will be quickly decomposed to NO. In the end, the composition of the NO_y generated from nitrate photolysis is still unknown exactly, however, NO_2 has been pointed out as emission input in the present atmospheric chemistry model for polar region (Zatko *et al.*, 2016; Zatko *et al.*, 2013). While, in a laboratory experiment, it is reported that NO_2^- production by nitrate photolysis is dominated at lower temperatures in ice but not NO_2 production. Some models do not include the NO_2^- production, which should underestimate NO, HONO and OH production (Erbland *et al.*, 2015; Zatko *et al.*, 2016). Calculated results in Antarctica that the OH concentration becomes 6 times and the O_3 concentration becomes 1.8 times due to NO_y release from snowpack have been reported (Zatko *et al*., 2016).

This paper aims to investigate following two main points: 1) the composition of released NO_y, 2) most photo-reactive depth in snowpack. For these purposes, NO, NO_2 and HONO flux observation, passive sampling of NO_2 and HONO in snowpack, and pit observation of sun light intensity were carried out in coastal area of the Antarctica in a summertime.

3.2 Material and Method

3.2.1 Location

The measurements were conducted at H128 (69°23.584S°, 41°33.712E°) at about 100 km from Syowa Station in eastern Dronning Maud Land, East Antarctica during the 57th Japanese Antarctic Research Expedition (JARE57) for December 2015 to February 2016.

3.2.2 Continuous NO_y Measurement

A CAPS-NO_2 monitor with NO oxidizing unit (Shorelines Science, Japan, detection limit (D.L) : 20 pptv) was used for the measurements of atmospheric NO and NO_2, and an aqua-membrane-type denuder (ADAMD) HONO analyzer (Takenaka *et al.*, 2004) was used for the measurements for atmospheric HONO. CAPS-NO_2 monitor is a measuring device for only NO_2 concentration. In NO measurement, O_3 in oxidizing unit mixed with sample gas to oxidize NO to NO_2 for being measurable by the NO_2 analyzer (NO oxidizing mode). The difference of the values under NO oxidizing mode to under normal mode was defined as NO concentration. All instruments were located at an experimental hut. An ambient air sampling inlet was set up at 2 m height and about 25 m upwind of katabatic wind from the research community (or the experimental hut) to minimize the influence of local pollution, which was connected to the CAPS-NO_2 monitor and the HONO analyzer by Teflon tubes (o.d. 6 mm and i.d. 4 mm). During flux measurement, a chamber (Fig. 1) was set up at 50 m upwind of katabatic wind from the

experimental hut and installed on the snowpack to measure NO_y flux from snowpack surface, then the chamber inlet was connected to these analyzers through two parallel Teflon tubes (o.d. 6 mm and i.d. 4 mm) in order to reduce the pressure depression due to long tube. This chamber (volume: 0.32 m^3, base area: 0.81 m^2) made by Teflon sheet was connected to the air sampling inlet and the analyzers. Basically, we measured the air sample (background) from 2 m above ground level and from the chamber (chamber sample) alternately every 10 minutes.

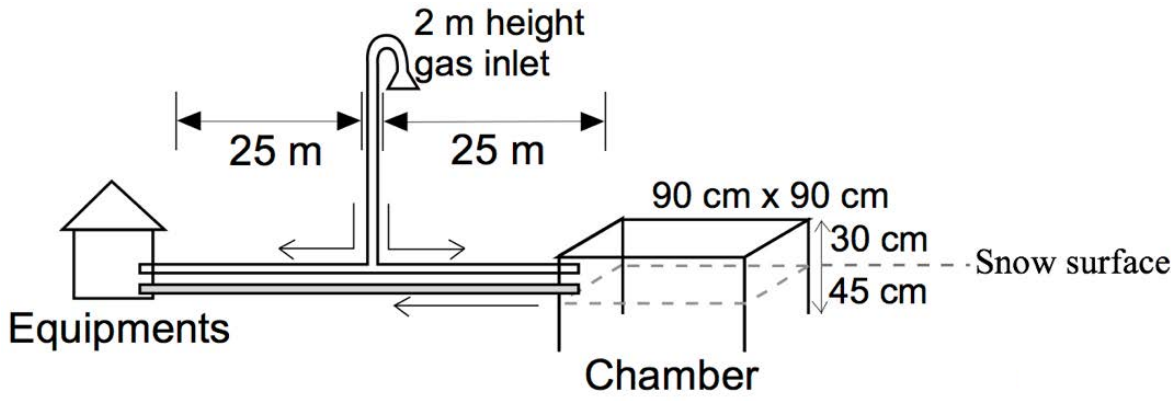

Fig.1 Schematic diagram of chamber.

3.2.3 Filter Pack Measurements

HNO_3, HONO and NH_3 gases were collected by a filterpack sampler (Noguchi *et al.*, 2007) with five stages. 1st filter is membrane filter (PTFE, 47 mm dia., pore size: 1.0 μm, ADVANTEC, Tokyo Japan) to remove particles, 2nd to 5th stage has paper filters (Filter paper 51A, 47 mmϕ, ADVANTEC, Tokyo Japan) with NaF, Na_2CO_3, Na_2CO_3, and H_3PO_4 as impregnating solution. The filter holder is a NILU filter holder inline system (Norwegian Institute for Air Research, Kjeller, Norway). Flow rate for sampling was 2 L

min^{-1}, which provides a sampling volume of approximately 3 m^3 day^{-1}. Filters were kept in clean bags at subzero temperature and brought back to the laboratory in Japan, and then ion concentrations were analyzed.

3.2.4 Passive Sampling in Snowpack

Passive samplers (TOHSEN, Japan) (Warashina *et al.*, 2001) for acidic gases in snowpack were used and set for 1 month (31 December, 2015 to 31 January, 2016) at 0, 5, 10, 20 and 40 cm depth. Filters were impregnated with Na_2CO_3, triethanolamine and NaF solution filters (Filter paper 51A, 26 mmϕ, ADVANTEC, Tokyo Japan) to collect acidic gases, NO_2 and HNO_3, respectively. Membrane filter was used as a cover filter (Membrane filter, 26 mmϕ, pore size: 1.0 μm, ADVANTEC). Three samplers were set at each depth. Filters were kept in clean bags at subzero temperature and brought back to the laboratory in Japan, and then ion concentrations were analyzed.

3.2.5 Ion Chromatograph Analysis

Trapped ions on filters were extracted by ultra-pure water (18.2 MΩ cm), and these extracts were analyzed by ion chromatography in laboratory. The anion chromatograph system (883 basic IC plus, Metrohm, Switzerland) had guard column (SI-90G, Shodex), separation column (SI-90 4E, Shodex), and suppressor for anions, and the eluent was a mixed solution of 1.8 mmol dm^{-3} Na_2CO_3 and 1.7 mmol dm^{-3} $NaHCO_3$ at 1 mL min^{-1} of flow rate. The cation chromatograph system (IC7000, YOKOGAWA) has separation

column (YS-50, Shodex) with eluent of 4 mmol dm^{-3} methanesulfonic acid at 1 mL min^{-1} of flow rate.

3.2.6 Sun Light Intensity Observation in Snowpack

Light intensity in the snowpack was observed with 1.3 m depth pit. An optical fiber spectrophotometer system with a UV/Vis probe (Ocean Optics TP300-UV/VIS probe and USB2000+UV-VIS-ES) was used for the observation. The tip of the probe with a right angle prism (Fig. 2) inserted up to 75 cm from the side of the pit wall at 10, 20, 30, 50, 75, 100 cm depth. In order to measure the light intensity from all directions in the snow, the probe was rotated 360° every 45° during the measurement.

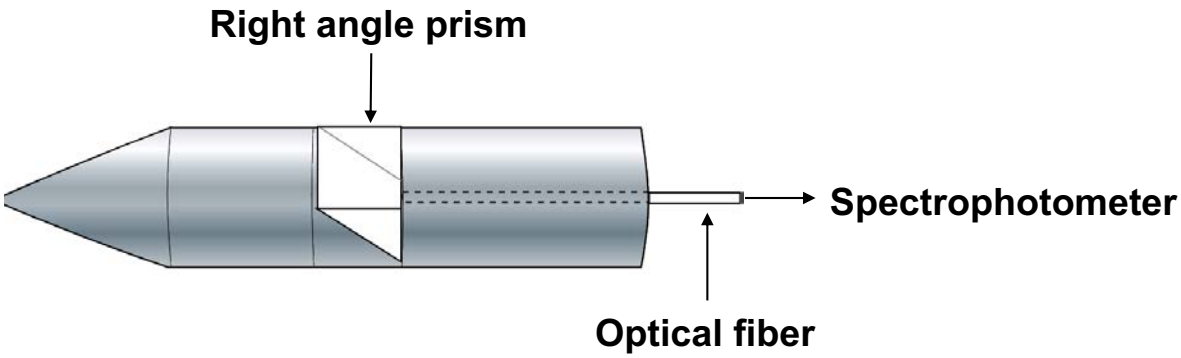

Fig. 2 Schematic diagram of light observation probe in snowpack.

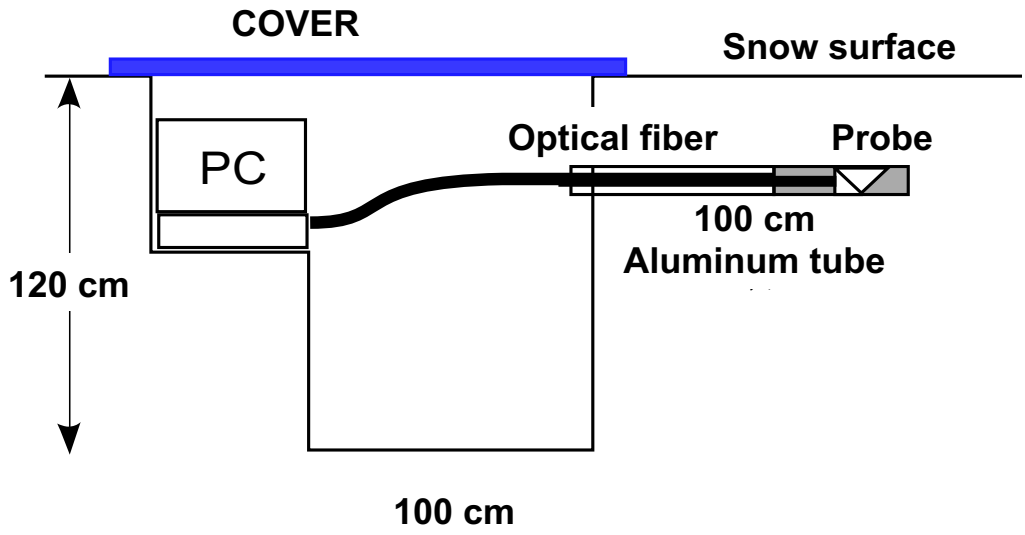

Fig. 3 Schematic diagram of light intensity observation with pit

3.2.7 AWS Installation

An automated weather station (AWS) was installed near the sampling site on 31st December 2015. The AWS measures air temperature and relative humidity by thermo-hygrometers (HMP-155, Vaisala, Finland, and multi-plate radiation shield model-41001, Young Co., USA), air pressure by a barometer (PTB210, Vaisala, Finland), wind speed

and direction by an aerovane (model-05130, Young Co., USA) and downward and upward solar radiation by a net radiometer (CNR-4, Kipp & Zonen, Netherland). The electrical power is supplied from cyclone batteries in the snow, which are charged by solar panels. For all instruments, 1-min sampling and 10-min averaged data are stored on a data logger, and 10-min averaged data are also transported via the Argos satellite.

3.2.8 Snow pit sampling for nitrate isotopic analysis

A pit was dug to take snow samples every 20 cm until 180 cm depth. The samples were measured for ion concentrations and isotopic compositions. (See 2.2.2)

3.3 Results and Discussion

3.3.1 NO_y Flux

The NO_2 gas concentration was observed using CAPS-NO_2 monitor. During the experimental period, NO_2 concentration was always less than detection limit (20 pptv) both of background and the chamber. $[NO]_{BG}$ and $[NO]_{cham}$ were observed from 12th to 27th (except 23th and 24th) January 2016 and 16th to 22nd January 2016, respectively. The brackets indicate concentration in pptv and the subscripts, BG and cham denote background and chamber, respectively. Fig. 4 shows the time series of $[NO]_{BG}$ and $[NO]_{cham}$. During the measurement period, the main wind direction of the katabatic wind was about 180 degrees (south).

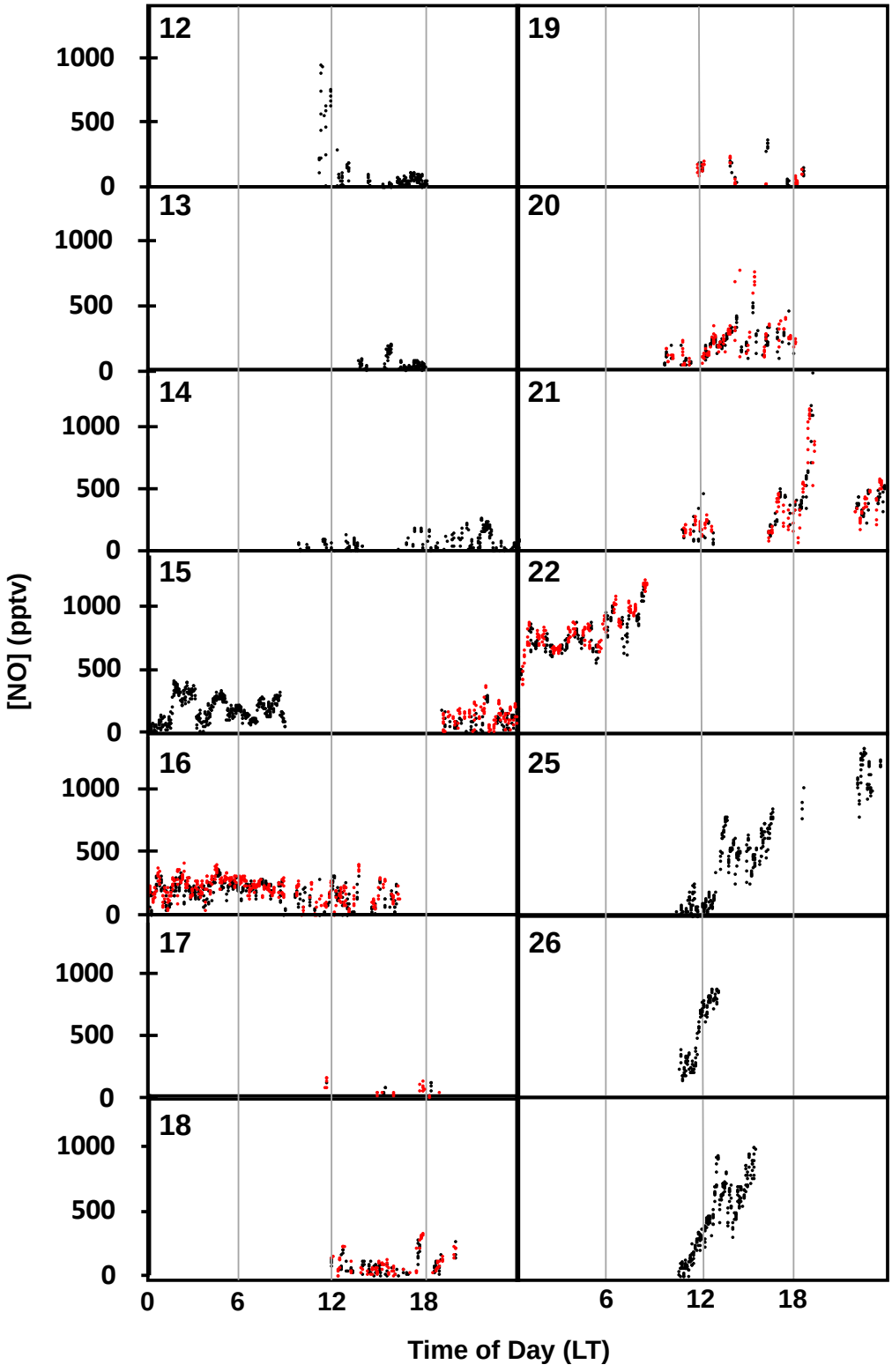

Fig. 4 Time series of $[NO]_{BG}$ (black) and $[NO]_{cham}$ (red). For atmospheric NO; Maximum: 1374.1 pptv, Average: 394.7 pptv.

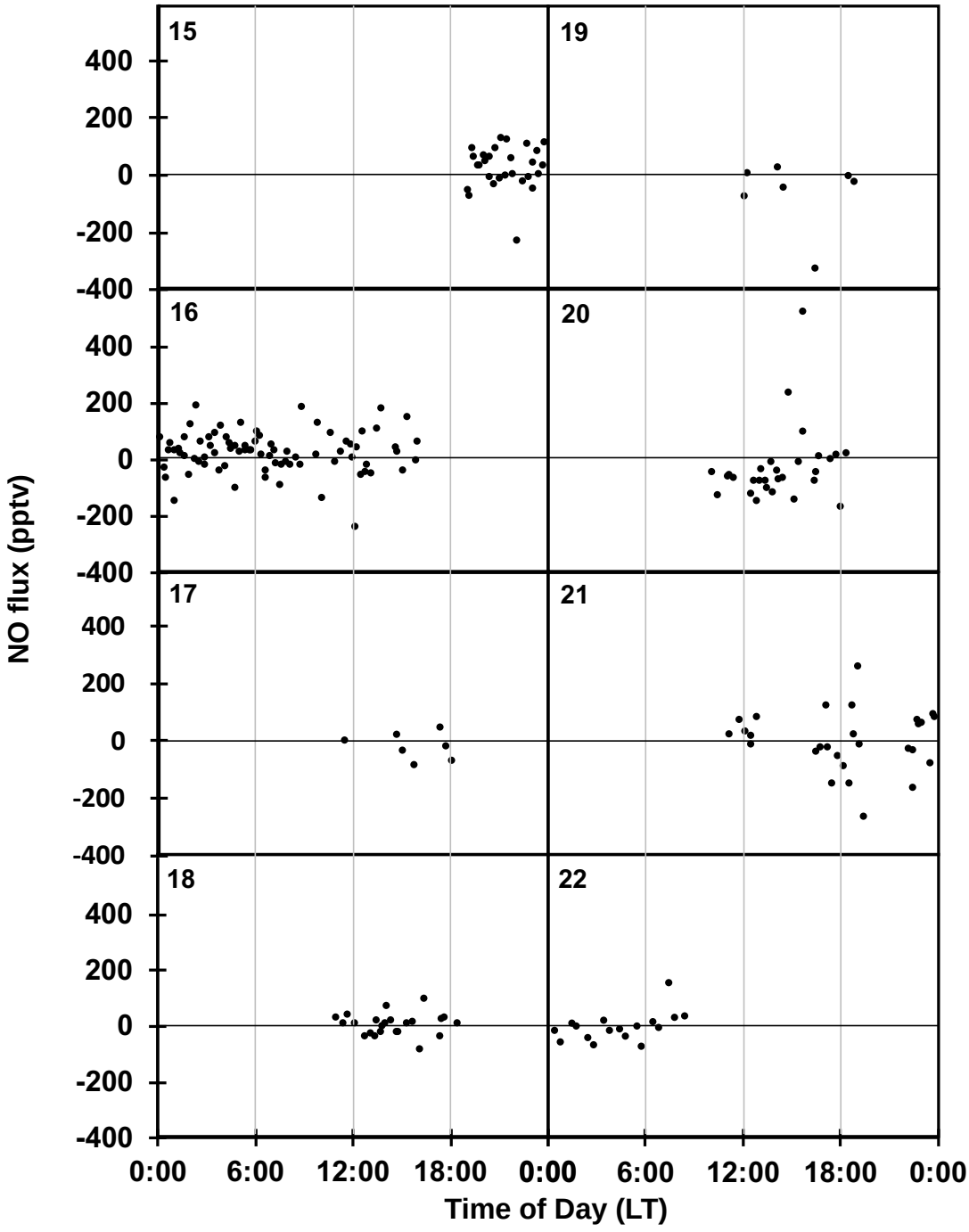

Fig. 5 Time series of NO flux. Maximum: 536.8 pptv, Average: 22.2 pptv.

In order to avoid contamination from research community, only the data that wind direction is within 100 to 250 degrees was used for analysis. Furthermore, the data that wind speed is less than 3 m is also excluded to avoid the contamination. Relatively high $[NO]_{BG}$ and $[NO]_{cham}$ were observed on days 22, 23 and 25. Maximum $[NO]_{BG}$, average $[NO]_{BG}$, maximum $[NO]_{cham}$ and average $[NO]_{cham}$ were 1227.8, 355.3, 277.7 and 1173.1 pptv, respectively. The order of the results was agree with the previous result in Antarctica (Davis *et al.*, 2004). While, any diurnal cycle that were common in all periods was not observed for $[NO]_{BG}$ and $[NO]_{cham}$. As we mentioned, $[NO]_{BG}$ and the $[NO]_{cham}$ were analyzed alternately. The NO flux was defined as the difference of $[NO]_{BG}$ and $[NO]_{cham}$ value. Thus, NO flux can be calculated on the day when $[NO]_{BG}$ and $[NO]_{cham}$ were measured at the same time, *i.e.* from 16th to 22nd January 2016. Figure 5 shows the time series of NO flux. There is also no diurnal cycle was observed for [NO] flux. The maximum NO flux and the average were 536.8 and 22.2 pptv, respectively. It indicates that NO is released from snowpack surface in the chamber. Both of $[NO]_{BG}$ and NO flux had no correlation with temperature, humidity, sunlight intensity and wind direction. Therefore, another factor such as a movement of the gas convection in firn would contribute to NO flux, the $[NO]_{BG}$ and $[NO]_{cham}$. $[HONO]_{BG}$ and $[HONO]_{cham}$ were observed from 8th to 26th January 2016. In the same manner as NO, $[HONO]_{BG}$, $[HONO]_{cham}$ and HONO flux are shown in Figs. 6 and 7.

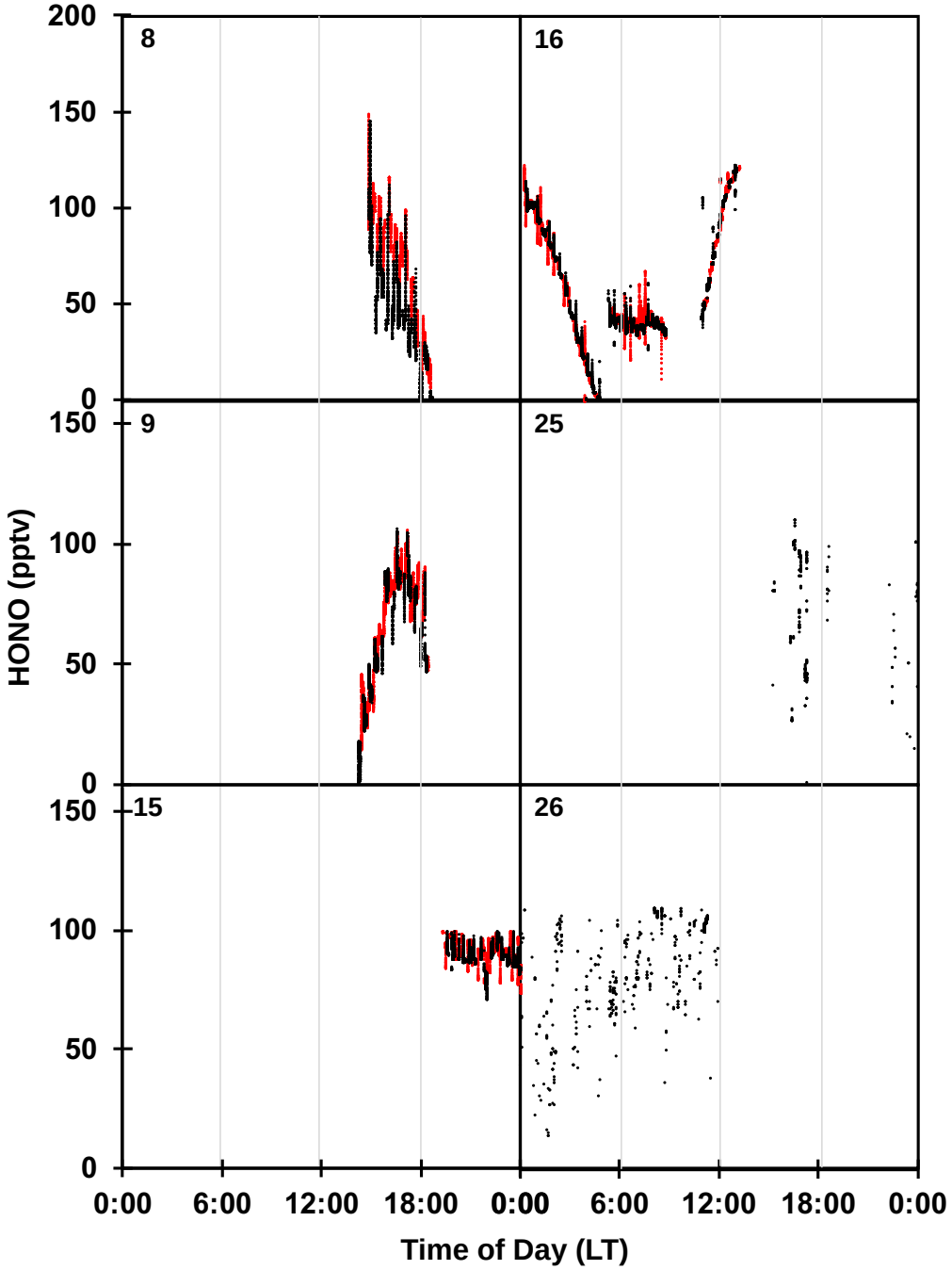

Fig. 6 Time series of $[HONO]_{BG}$ (black) and $[HONO]_{cham}$ (red) For$[HONO]_{BG}$: Maximum: 144.7 pptv, Average: 57.6 pptv.

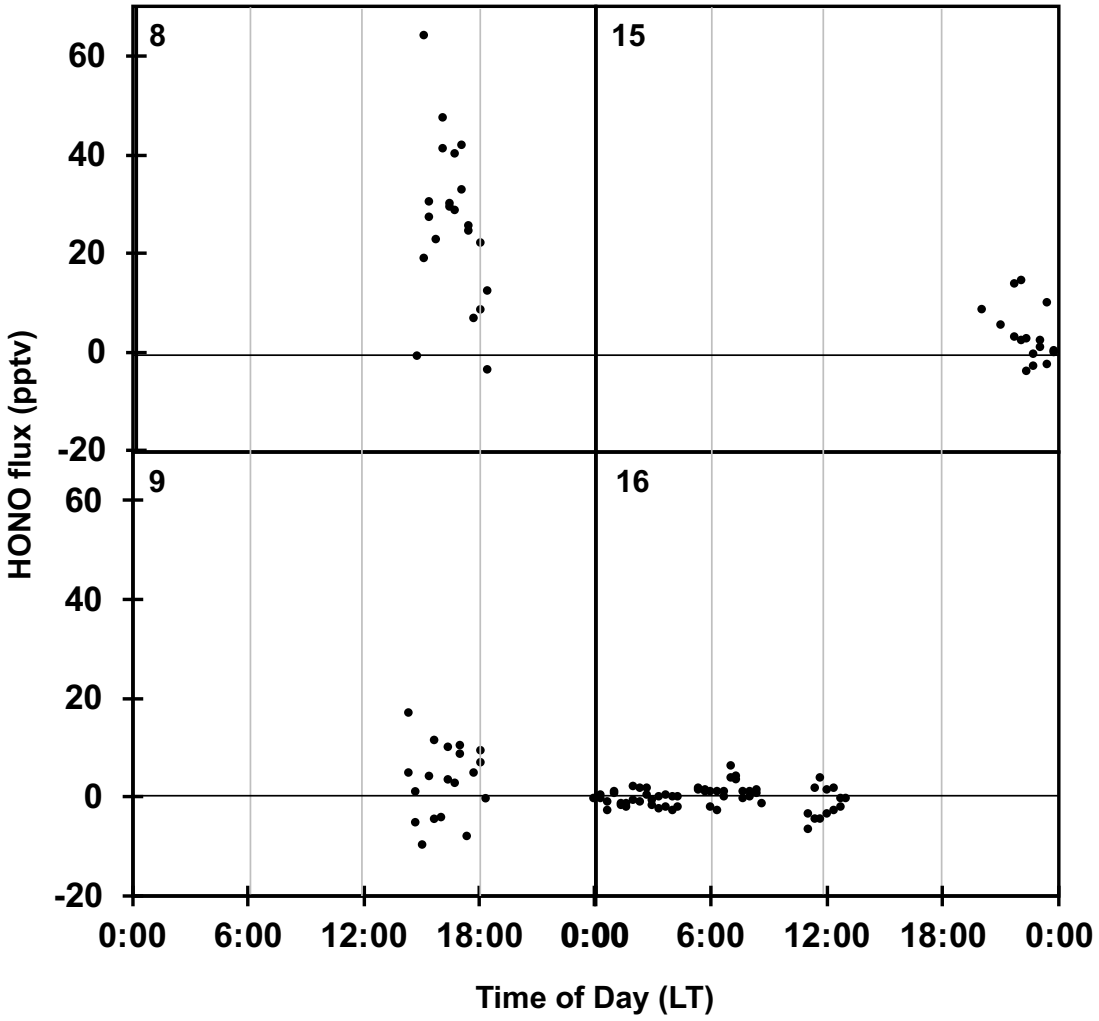

Fig. 7 Time series of HONO flux. Maximum: 64.4 pptv, Average: 12.2 pptv.

$[HONO]_{cham}$ has higher values than $[HONO]_{BG}$, indicating that HONO is released from the snowpack surface. From the HONO flux on 8th January 2016, a sharp peak was obswerved at around 16:00, suggesting involvement with solar light intensity. However, such trends were not observed on other days, thus it is unknown what is the dominant

factor of HONO flux. Maximum $[HONO]_{BG}$, average $[HONO]_{BG}$, maximum $[HONO]_{cham}$, average $[HONO]_{cham}$ and HONO flux was 144.7, 57.6, 63.9, 149.2 and 12.2 pptv, respectively. Average $[NO]_{BG}$ was 6 times higher than average $[HONO]_{BG}$, since HONO released form snowpack surface is rapidly photodecomposed to NO in the atmosphere. $[HONO]_{BG}$ and HONO flux also had no correlation with weather conditions. Therefore, we concluded that the NO_y flux is controlled by the convection in firn. While, the flux ratio of NO : HONO : NO_2 was approximately 2 : 1 : 0. Atmospheric environment with no NO_2 and high [HONO] has never been reported from any area in the Antarctica. We used CAPS NO_2 monitor for the observation of NO and NO_2, which is an important difference from the previous researches. This is because CAPS NO_2 monitor directly measures the NO_2 concentration, thus the value of NO_2 concentration measured by CAPS NO_2 monitor is reliable. On the other hand, chemiluminescence method which measure NO directly and measure NO_2 with molybdenum reduction converter has been used for NO and NO_2 observations in previous studies, possibly overestimating NO_2. According to the previous study, since NO_2^- production dominates at low temperatures in ice (Benedict & Anastasio, 2017), HONO was produced more than NO_2. To draw a conclusion on this question, further observation and simulation studies are necessary. The new finding will contribute to the improvement of the accuracy of the Antarctic nitrogen circulation model.

3.3.2 Filter Pack Results

The results of $[HNO_3]_{BG}$, $[HNO_3]_{cham}$, $[HONO]_{BG}$, and $[HONO]_{cham}$ collected by filter pack method are shown in Table 1. Since HNO_3 is stickyc, HNO_3 gas would be adsorbed on the inner wall of the tubes leading underestimating. Although it was not measured simultaneously with the continuous method (NO_y flux measurement), since the order of HONO continuous data and its filter pack method are in agreement, the value of continuous measurement is considered to be reliable. Furthermore, since the [HONO] value of the chamber is higher than its atmospheric value, it agrees with our positive flux observation using continuous methods. On the other hand, the results of the dark chamber measured by the filter pack method are valuable and suggestive. High concentration of HONO was detected in the chamber shielded by aluminum plate up to 90 cm depth. In addition, the light intensity at 310 nm, which is important for nitrate photolysis, at 80 cm depth was half as strong as its at 10 cm depth as shown in Fig. 8. It has been pointed out that photic zone at Dome C in Antarctica is approximately 10 cm in the previous laboratory experiment (Anastasio and Robles, 2007), however, our observation is conducted not in laboratory but in the field. That is, there is a possibility that the depth at which nitrate photolysis occurs is deeper than the experimental prediction. This hypothesis is also suggested from the results of the passive sampler described at next section.

Table 1 [HNO_3] and [HONO] collected by filter pack method during January 2016.

**The results obtained under dark condition. The chamber was shielded from light by aluminum plate until 90 cm depth.*

Date	$[HNO_3]_{BG}$	$[HNO_3]_{cham}$	$[HONO]_{BG}$	$[HONO]_{cham}$
	(pptv)			
10 to 12	123.0	41.0	48.5	113.1
13 to 15	57.0	11.4	238.6	80.9
23	159.6	21.8	28.0	57.8
22 to 23	0.0	0.0*	20.1	66.7*
24	0.0	125.2	13.5	57.8
25	108.5		60.9	
26	0.0		1.0	
27	0.0		22.7	

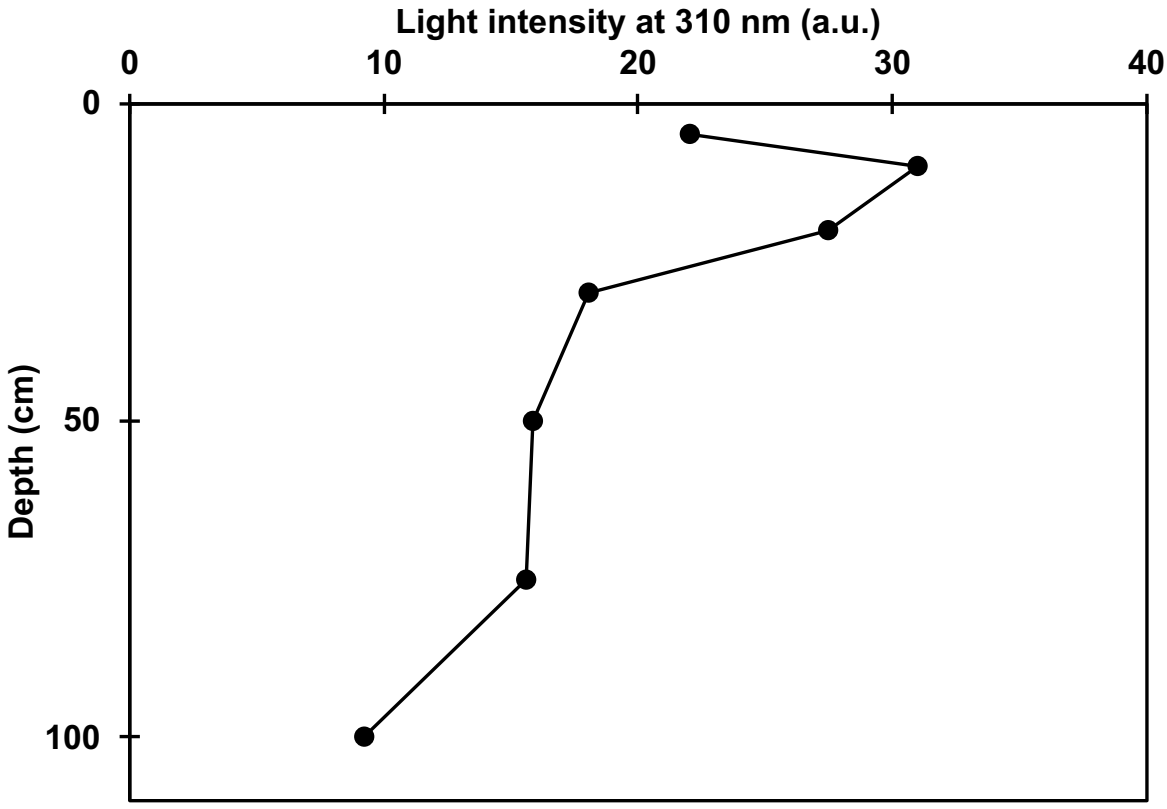

Fig. 8 Depth profile of light intensity at 310 nm in snowpack.

3.3.3 Depth Profile of HONO by Passive Sampling in Snowpack

Fig. 9 shows the amount of NO_2^- trapped on the passive sampler in the snowpack. No NO_2^- was trapped on NaF impregnated filters. For TEA impregnated filters, NO_2^- was trapped on only 40 cm depth filter. On the Na_2CO_3 impregnated filters, more deeply in the snow, more NO_2^- was collected on the filters. It seems that NaF and TEA could not sufficiently adsorb NO_2^- because of its weak alkalinity. Since NO_2 gas was not detected in the atmosphere as we mentioned, it is unlikely that NO_2 is present in firn air. Therefore, the NO_2^- collected by the passive samplers would be derived from HONO. Our result shows that nitrate photolysis would progress in the deep snow which generate HONO. This result contributes to the improvement of the precision of snow chemistry model and atmospheric chemistry model. In addition, this result supports our hypothesis which NO_y generated form nitrate is retained in firn and is released by convection in snowpack.

Since NO_2 was not detected, the primary product from nitrate photolysis in the snowpack is HONO. Furthermore, HONO as a primary product is photo decomposed to produce NO. In the conventional Antarctic nitrogen circulation model, NO and NO_2 were regarded as the main products of nitrate photolysis. From the model, ozone production by a photochemical reaction of NO_2 was suggested. However, if HONO rather than NO_2 was generated, OH radicals rather than O_3 would be the main oxidant in firn. Whether O_3 or OH is dominant, the difference significantly affects the lifetime of other chemical substance such as halogens and organics (Domine and Shepson, 2002). Therefore, our results that HONO is primary produced by nitrate photolysis and released by convection in the snowpack with secondary products have a great impact on the Antarctic

atmospheric chemistry.

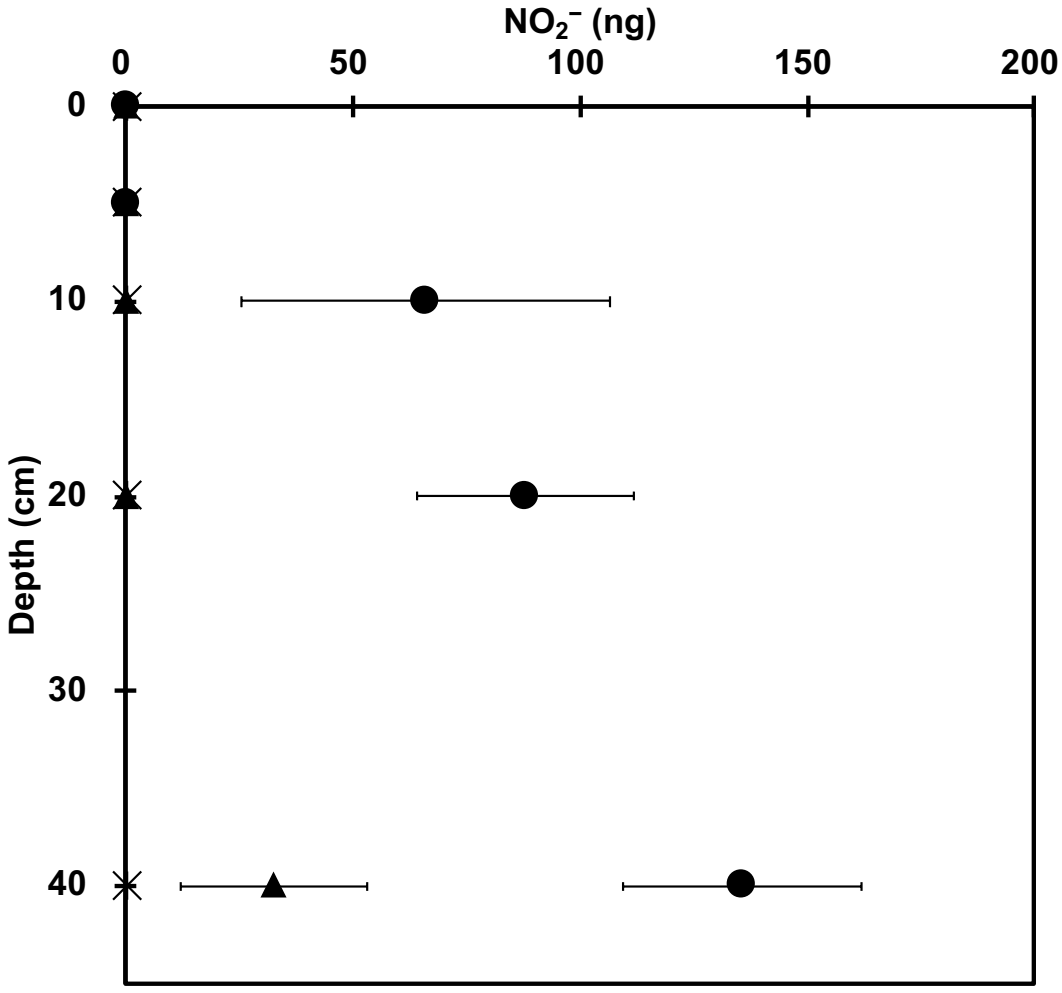

Fig. 9 Depth profile of HONO by passive sampler during 31 December, 2015 to 31 January, 2016. n=3, error bar is one-σ. The types of plots show impregnating liquid (asterisks: NaF, triangles: TEA and circles: Na_2CO_3).

3.3.4 Vertical profile of $\delta^{15}N(NO_3^-)$

Fig. 10 shows a vertical profile of $\delta^{15}N(NO_3^-)$. $\delta^{15}N(NO_3^-)$ weighted average of

surface snow at coastal sites (S30, H42, H68, H88, H108 and H128) is calculated to –9.8 ± 11 ‰ which is considered to an initial value of $\delta^{15}N(NO_3^-)$ in coastal sites (data taken from Section 2.2.2, Table 1). This $\delta^{15}N(NO_3^-)$ is lower than the nitrate derived from the stratosphere (19 ‰). This is because $^{14}NO_3^-$ takes precedence over $^{15}NO_3^-$ when nitrate is re-released to the atmosphere by photolysis, so that in the coastal area, the $\delta^{15}N(NO_3^-)$ is lower than that in the inland area. As mentioned in Section 2.4.1, enrichment of $\delta^{15}N(NO_3^-)$ would be due to the nitrate photolysis, thus the $\delta^{15}N(NO_3^-)$ values of Fig. 10 lower than –9.8 ± 11 ‰ imply progress of nitrate photolysis in costal snowpack. Furthermore, since at deeper places the $\delta^{15}N(NO_3^-)$ enrichment is significant, there is a possibility that nitrate photolysis may proceed even in the deep snow, which is also consistent with the result of passive sampling (Section 3.3.3). However, NO_y produced by nitrate photolysis in snowpack should have lower $\delta^{15}N(NO_3^-)$. The NO_y is not immediately released to the atmosphere but convects in the firn. Since NO_y moves within firn and may be deposited as nitrate on snow again, it is difficult to determine the dynamics of nitrate only from $\delta^{15}N(NO_3^-)$ and its initial value. At least $\delta^{15}N(NO_3^-)$ lower than the initial value cannot be explained without contribution of photolysis.

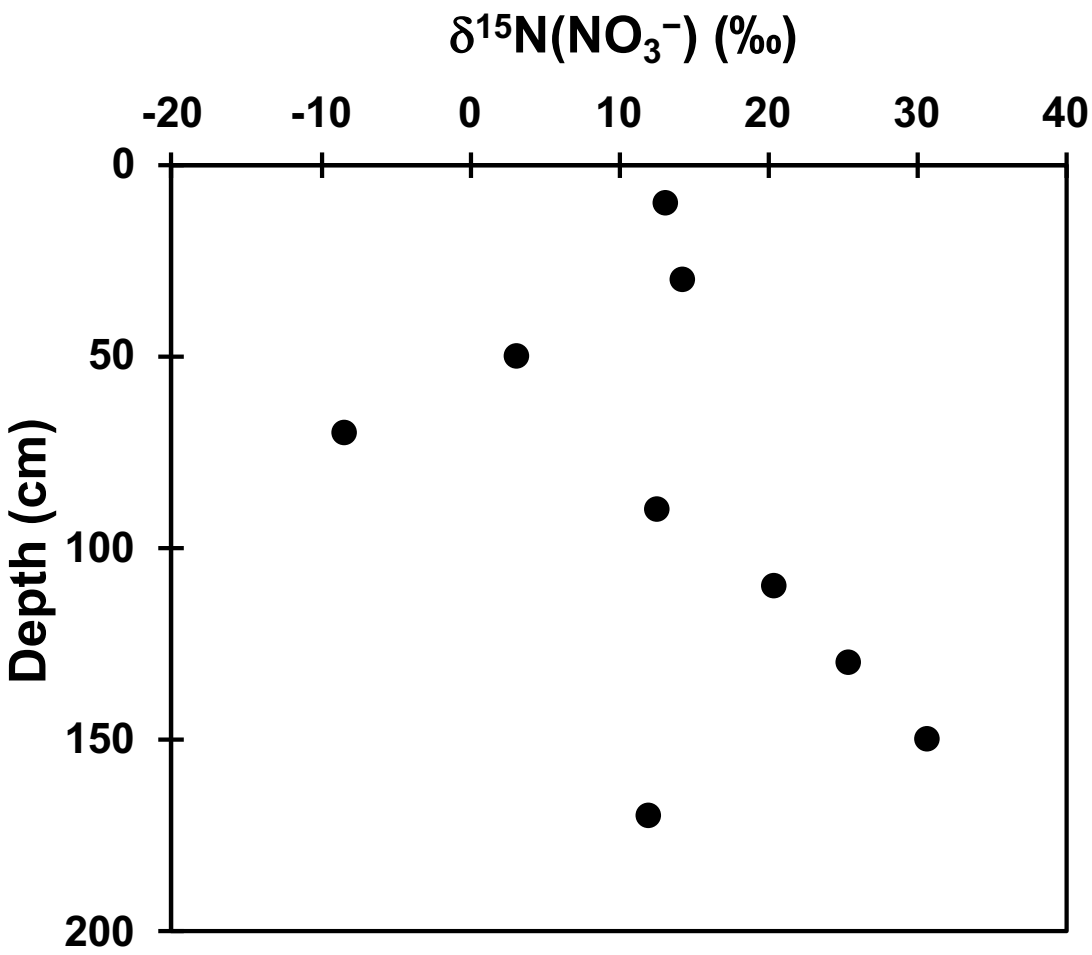

Fig. 10 Vertical profile of $\delta^{15}N(NO_3^-)$

3.4 Conclusion

We provided observation data of background NO_y concentration, NO_y flux from snowpack surface, and depth profile of HONO in the snowpack in the coastal site in the Antarctica. NO_2 was not detected both in the atmosphere and from snowpack. We concluded that the difference between previous data and our data was due to the difference in measuring equipment. Previous studies that measured NO_2 using the chemiluminescence method may possibly overestimate NO_2. Our results suggested that the primary product from nitrate photolysis is HONO and the secondary product is NO. In addition, from the results of the passive sampler and flux from dark chamber, nitrate photolysis would be progressed in the deep snow about 1 m. This hypothesis is also supported by depth profile of $\delta^{15}N(NO_3^-)$.

References

Amoroso, A., Beine, H. J., Sparapani, R., Nardino, M. and Allegrini, I. (2006). Observation of coinciding arctic boundary layer ozone depletion and snow surface emissions of nitrous acid. *Atmos. Environ.*, *40*(11), 1949-1956. doi:https://doi.org/10.1016/j.atmosenv.2005.11.027

Anastasio, C. and Robles, T. (2007). Light absorption by soluble chemical species in Arctic and Antarctic snow. *J. Geophys. Res.-Atmos, 112*(24), D24304. doi:10.1029/2007JD008695

Beine, H. J., Amoroso, A., Dominé, F., King, M. D., Nardino, M., Ianniello, A. and France, J. L. (2006). Surprisingly small HONO emissions from snow surfaces at Browning Pass, Antarctica. *Atmos. Chem. Phys.*, *6*(9), 2569-2580. doi:10.5194/acp-6-2569-2006

Benedict, K. B. and Anastasio, C. (2017). Quantum Yields of Nitrite (NO_2^-) from the Photolysis of Nitrate (NO_3^-) in Ice at 313 nm. *J. Phys. Chem. A, 121*(44), 8474-8483. doi:10.1021/acs.jpca.7b08839

Blunier, T., Floch, G. L., Jacobi, H.-W. and Quansah, E. (2005). Isotopic view on nitrate loss in Antarctic surface snow. *Geophys. Res. Lett.*, *32*(13), L13501. doi:10.1029/2005GL023011

Boxe, C. S., Colussi, A. J., Hoffmann, M. R., Murphy, J. G., Wooldridge, P. J., Bertram, T. H. and Cohen, R. C. (2005). Photochemical Production and Release of Gaseous NO_2 from Nitrate-Doped Water Ice. *Phys. Chem. A, 109*(38), 8520-8525. doi:10.1021/jp0518815

Clemitshaw, K. C. (2006). Coupling between the Tropospheric Photochemistry of Nitrous Acid (HONO) and Nitric Acid (HNO_3). *Environmental Chemistry, 3*(1), 31-34. doi:https://doi.org/10.1071/EN05073

Davis, D., Chen, G., Buhr, M., Crawford, J., Lenschow, D., Lefer, B. and Hogan, A. (2004). South Pole NOx Chemistry: an assessment of factors controlling variability and absolute levels. *Atmos. Environ., 38*(32), 5375-5388. doi:https://doi.org/10.1016/j.atmosenv.2004.04.039

Domine, F. and Shepson, P. (2002). Air-Snow Interactions and Atmospheric Chemistry. *Science, 297*, 1506-1510. doi:10.1126/science.1074610

Erbland, J., Savarino, J., Morin, S., France, J. L., Frey, M. M. and King, M. D. (2015). Air–snow transfer of nitrate on the East Antarctic Plateau – Part 2: An isotopic model for the interpretation of deep ice-core records. *Atmos. Chem. Phys., 15*(20), 12079-12113. doi:10.5194/acp-15-12079-2015

Frey, M. M., Savarino, J., Morin, S., Erbland, J. and Martins, J. M. F. (2009). Photolysis imprint in the nitrate stable isotope signal in snow and atmosphere of East Antarctica and implications for reactive nitrogen cycling. *Atmos. Chem. Phys., 9*(22), 8681-8696. doi:10.5194/acp-9-8681-2009

Grannas, A. M., Hockaday, W. C., Hatcher, P. G., Thompson, L. G. and Mosley-Thompson, E. (2006). New revelations on the nature of organic matter in ice cores. *J. Geophys. Res.-Atmos, 111*(D4), D04304. doi:10.1029/2005JD006251

Honrath, R. E., Lu, Y., Peterson, M. C., Dibb, J. E., Arsenault, M. A., Cullen, N. J. and Steffen, K. (2002). Vertical fluxes of NOx, HONO, and HNO_3 above the

snowpack at Summit, Greenland. *Atmos. Environ.*, *36*(15), 2629-2640. doi:https://doi.org/10.1016/S1352-2310(02)00132-2

Honrath, R. E., Peterson, M. C., Guo, S., Dibb, J. E., Shepson, P. B. and Campbell, B. (1999). Evidence of NOx production within or upon ice particles in the Greenland snowpack. *Geophys. Res. Lett.*, *26*(6), 695-698. doi:10.1029/1999GL900077

Jacobi, H.-W. and Hilker, B. (2007). A mechanism for the photochemical transformation of nitrate in snow. *J. Photoch. Photobio. A*, *185*(2), 371-382. doi:https://doi.org/10.1016/j.jphotochem.2006.06.039

Jones, A. E., Weller, R., Anderson, P. S., Jacobi, H. W., Wolff, E. W., Schrems, O. and Miller, H. (2001). Measurements of NOx emissions from the Antarctic snowpack. *Geophys. Res. Lett.*, *28*(8), 1499-1502. doi:10.1029/2000GL011956

Kleffmann, J. and Wiessen, P. (2008). Technical Note: Quantification of interferences of wet chemical HONO LOPAP measurements under simulated polar conditions. *Atmos. Chem. Phys.*, *8*(22), 6813-6822. doi:10.5194/acp-8-6813-2008

Legrand, M., Preunkert, S., Frey, M., Bartels-Rausch, T., Kukui, A., King, M. D. and Jourdain, B. (2014). Large mixing ratios of atmospheric nitrous acid (HONO) at Concordia (East Antarctic Plateau) in summer: a strong source from surface snow? *Atmos. Chem. Phys.*, *14*(18), 9963-9976. doi:10.5194/acp-14-9963-2014

Liao, W., Case, A. T., Mastromarino, J., Tan, D. and Dibb, J. E. (2006). Observations of HONO by laser-induced fluorescence at the South Pole during ANTCI 2003. *Geophys. Res. Lett.*, *33*(9), L09810. doi:10.1029/2005GL025470

Mack, J. and Bolton, J. (1999). Photochemistry of nitrite and nitrate in aqueous solution:

A review. J. Photochem. Photobio. A, (128), 1-13.

Meusinger, C., Berhanu, T. A., Erbland, J., Savarino, J. and Johnson, M. S. (2014). Laboratory study of nitrate photolysis in Antarctic snow. I. Observed quantum yield, domain of photolysis, and secondary chemistry. *J. Chem. Phys.*, *140*(24), 244305. doi:10.1063/1.4882898

Noguchi, I., Otsuka, H., Akiyama, M., Sakai, S. and Kato, T. (2007). Measuring Concentrations of Nitrous Acid Gas by the Filter-Pack Sampling Method. *Journal of Japan Society for Atmospheric Environment / Taiki Kankyo Gakkaishi, 42*(3), 162-174. doi:10.11298/taiki1995.42.3_162

Röthlisberger, R., Hutterli, M. A., Sommer, S., Wolff, E. W. and Mulvaney, R. (2000). Factors controlling nitrate in ice cores: Evidence from the Dome C deep ice core. *J. Geophys. Res.-Atmos, 105*(D16), 20565-20572. doi:10.1029/2000JD900264

Sumner, A. L. and Shepson, P. B. (1999). Snowpack production of formaldehyde and its effect on the Arctic troposphere. *Nature, 398*, 230. doi:10.1038/18423

Takenaka, N., Terada, H., Oro, Y., Hiroi, M., Yoshikawa, H., Okitsu, K. and Bandow, H. (2004). A new method for the measurement of trace amounts of HONO in the atmosphere using an air-dragged aqua-membrane-type denuder and fluorescence detection. *Analyst, 129*(11), 1130-1136. doi:10.1039/b407726a

Warashina, M., Tanaka, M., Tsujino, Y., Mizoguchi, T., Hatakeyama, S. and Maeda, Y. (2001). Atmospheric Concentrations of Sulfur Dioxide and Nitrogen Dioxide in China and Korea Measured by Using the Improved Passive Sampling Method. *Water, Air, Soil Pollut., 130*(1), 1505-1510. doi:10.1023/A:1013941820431

Zatko, M., Erbland, J., Savarino, J., Geng, L., Easley, L., Schauer, A., Bates, T., Quinn, P. K., Light, B., Morison, D., Osthoff, H. D., Lyman, S, Neff, W., Yuan, B. and Alexander, B. (2016). The magnitude of the snow-sourced reactive nitrogen flux to the boundary layer in the Uintah Basin, Utah, USA. *Atmos. Chem. Phys.*, *16*(21), 13837-13851. doi:10.5194/acp-16-13837-2016

Zatko, M. C., Grenfell, T. C., Alexander, B., Doherty, S. J., Thomas, J. L. and Yang, X. (2013). The influence of snow grain size and impurities on the vertical profiles of actinic flux and associated NOx emissions on the Antarctic and Greenland ice sheets. *Atmos. Chem. Phys.*, *13*(7), 3547-3567. doi:10.5194/acp-13-3547-2013

Zhou, X., Beine, H. J., Honrath, R. E., Fuentes, J. D., Simpson, W., Shepson, P. B. and Bottenheim, J. W. (2001). Snowpack photochemical production of HONO: A major source of OH in the Arctic boundary layer in springtime. *Geophys. Res. Lett.*, *28*(21), 4087-4090. doi:10.1029/2001GL013531

Chapter 4: Photolysis and Sublimation as Post-depositional Loss of Nitrate and Chloride in Snow

4.1 Introduction

Nitrate in snow is subject to post-depositional processing which leads to net loss and redistribution within the snowpack (Frey *et al.*, 2009; Jacobi and Hilker, 2007; Röthlisberger *et al.*, 2000). The relative importance of post-depositional loss processes, *i.e*. volatilization of nitric acid (HNO_3) and photolysis of nitrate, has long been debated (Blunier *et al.*, 2005; Röthlisberger *et al.*, 2000). Nitrate photolysis in/on snowpack has been known as a source of NO_y in the atmosphere (Honrath *et al.*, 1999; Jones *et al.*, 2001). While the photochemistry of nitrate in the snowpack has significant implications since its photoproducts, NO, NO_2 and radicals, are intimately linked to reactions involving ozone, hydrocarbons and halogens.

Nitrate undergoes photolysis in quasi liquid layer of ice, then NO_2 (Eq. 1) or NO_2^- (Eq. 2) is produced (Grannas *et al.*, 2006; Mack and Bolton, 1999; Meusinger *et al.*, 2014).

$$NO_3^- + h\nu + H^+ \rightarrow NO_2 + OH \qquad (R1)$$

$$NO_3^- + h\nu \rightarrow NO_2^- + O(^3P) \qquad (R2)$$

Nitrate in ice cores is a potential proxy for NO_y levels in the atmosphere of the past (Dibb *et al.*, 1998). Solar variability on centennial to millennial time scales may imprint on the long-term NO_3^- record, as suggested by Traversi *et al.* (2012) in their work on the Talos Dome core record. Traversi *et al.* argued that traces of solar variability remain as nitrate in ice core drilled in high accumulation site (Traversi *et al.*, 2012), but doubts still remain (see section 2.4.3). Apart from that, volatilization of weak acid from ice surface has been reported. In previous study, nitric acid is not volatilized and hydrochloric acid is reported to be volatilized slowly (Sato *et al.*, 2008). By placing it longer than the

previous study, nitric acid and more hydrochloric acid will volatilize. This mechanism should have an effect on the geochemical cycle in Antarctica where snow exists for a long time. Laboratory experiments to verify the hypothesis are indispensable to settle these discussions, however, it is difficult to make the Antarctic environment in laboratory. On the other hand, in field work, the large uncertainty of the environment leads the difficulty to quantify the theory. Thus, experiments in real Antarctic environment as a laboratory is needed.

This study aims to investigate following two main points: 1) to quantify the chloride and nitrate post-depositional loss, 2) Determination of snow depth at which nitrate photolysis occurs.

4.2 Material and Method

4.2.1 Location

Post-depositional process experiments were conducted at H128 (69°23.584S°, 41°33.712E°) at about 100 km from Syowa Station in eastern Dronning Maud Land, East Antarctica during the 57th Japanese Antarctic Research Expedition (JARE57) for December 2015 to February 2016. In addition, Homogenization of snow sample experiments were conducted in Nagano, Rikubetsu, Gifu and H128.

4.2.2 Nitrate Volatilization from Ice Surface

Sample solutions (100 μM $NaNO_3$, pH: 2-5 adjusted by H_2SO_4, 100 mL) was run into petri dish (i.d. 95 mm). The dishes were kept in freezer at −20 or −60℃ for three weeks. After that, the samples were melted at room temperature to analyze by ion chromatograph.

4.2.3 Application of Quartation for Mixing Snow

A polyethylene sheet cleaned by ultra-pure water (18.2 MΩ cm) was placed on a metal frame (90 × 90 × 90 cm^3) to make a container. Surface snow was put into the container up to the half of it (Fig. 1). The snow sample was smoothed and divided into four parts. Unmixed blank samples were collected from centers of whole sample and the divided parts (Fig. 2). Subsequently, the divided samples were mixed at diagonals or oppositional three times (mixed sample) as shown in Fig. 3, called quartation in soil science. Mixed sample was divided into four parts again to collect mixed blank samples

from centers of whole sample and the divided parts (Soil microbial experiment method, 1977).

Fig. 1 Snow sample in container

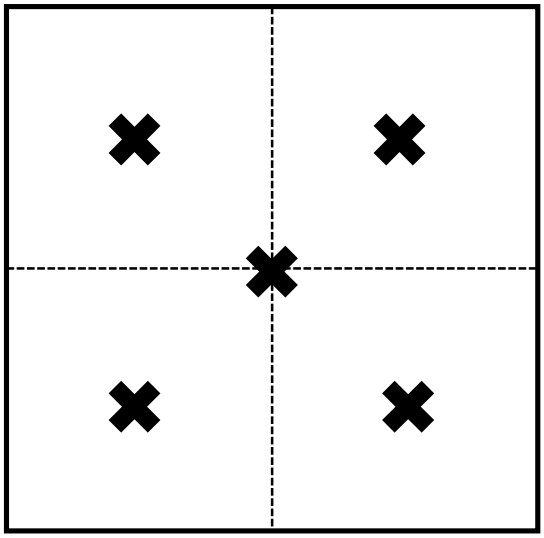

Fig. 2 Blank sample collection point

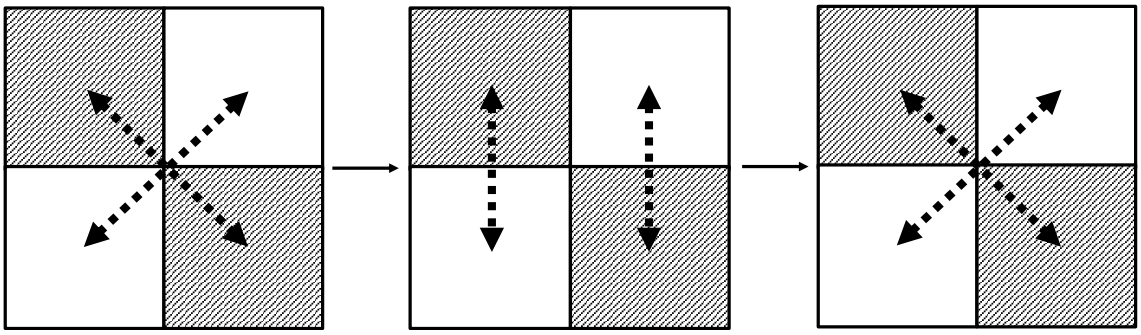

Fig. 3 Quartation mixing step

4.2.4 Natural Sample Preparation and Sampling in Field

The sample mixed by quartation method was packed in Teflon coated glass tubes (i.d. 5 cm length 40 cm) which buried in snowpack under three conditions for four weeks. First condition is the most natural condition, just burying the glass tubes in snowpack (OPEN condition). In the second condition, glass beakers were placed on top of the glass tubes to prevent deposition on the sample (COVERED condition). At that time, a gap for allowing air to pass through was secured. Under the third condition, an aluminum tape was wrapped around glass tubes to shield the sunlight, then glass beakers also wrapped with aluminum tape was placed on the glass tube with gap as well as second condition (DARK condition). Every week, three glass tubes of each condition were taken out the sample was cut every 5 cm. Before and after sampling, the sample in the glass tubes were weighed out to calculate sample density (0.50 g cm^{-3}). The cut samples were stored in clean bags and brought back in frozen state.

4.2.5 Amended Sample Preparation and Sampling in Field

The containers were set up as well as natural snow samples were prepared. 100 mL of NaCl, NH_4Cl, $NaNO_3$ 100 mM solution was sprayed on the snow sample. Subsequent mixing, glass tube packing, sampling procedures were the same as natural snow (amended sample).

4.2.6 Sun Light Intensity Observation in Snowpack

See in section 3.2.6

In addition, the reference was measured by placing the probe on 30 cm of a reflector (SRT-99-050, Labsphere) fixed at a height of 150 cm.

4.2.7 Temperature Observation in Snow

Thermocouples connected to thermorecorders (TR-72Ui, T&D corp.) were inserted in the snowpack at 0, 10, 20, 30 and 40 cm depth to measure temperature gradient in snowpack continuously (Fig. 4).

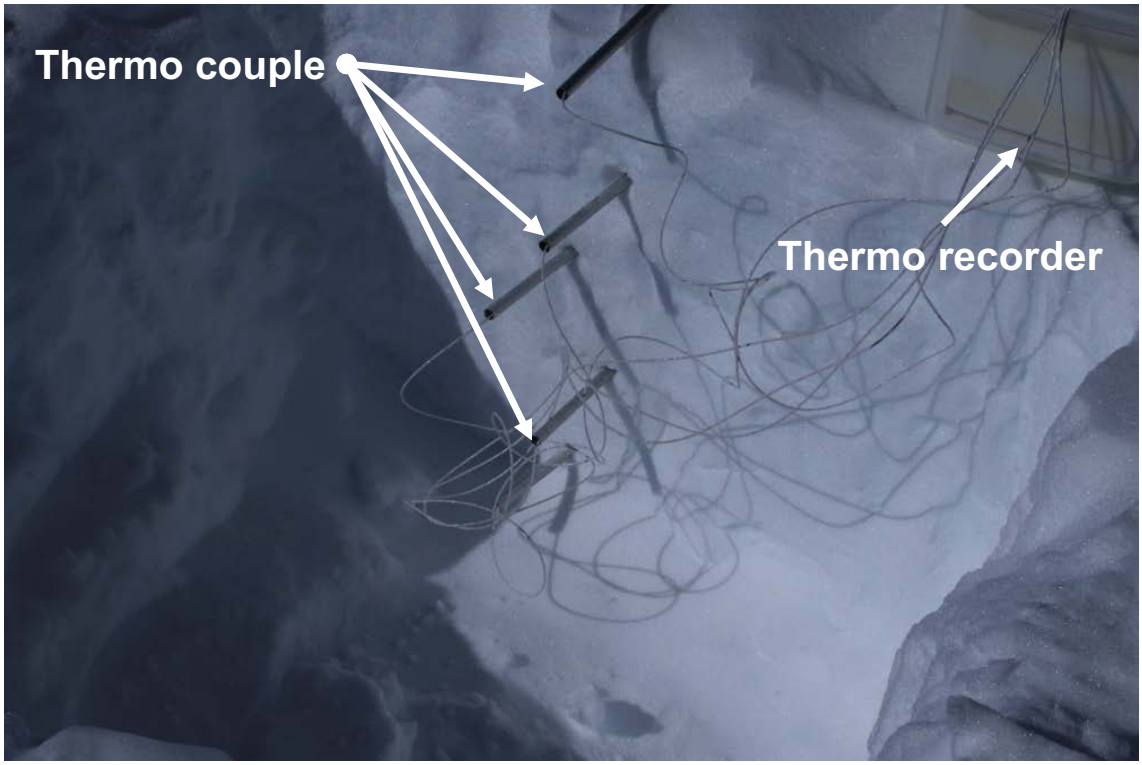

Fig. 4 Temperature observation in snowpack

4.2.8 Ion Chromatograph Analysis

Natural samples were analyzed by ion chromatography in laboratory. Amended samples were 20 times diluted with ultra-pure water. The anion chromatograph system (883 basic IC plus, Metrohm, Switzerland) had guard column (SI-90G, Shodex), separation column (SI-90 4E, Shodex), and suppressor for anions, and the eluent was a mixed solution of 1.8 mmol dm^{-3} Na_2CO_3 and 1.7 mmol dm^{-3} $NaHCO_3$ at 1 mL min^{-1} of flow rate. The cation chromatograph system (IC7000, YOKOGAWA) has separation column (YS-50, Shodex) with eluent of 4 mmol dm^{-3} methanesulfonic acid at 1 mL min^{-1} of flow rate.

4.3 Results and Discussion

4.3.1 Nitrate Volatilization from Ice Surface

Fig. 5 shows the decrement of nitrate concentration from ice surface for three weeks at −20 or −60℃. Since the apparent ion concentration changes with the evaporation of water, nitrate concentrations were standardized by [Na^+]. At −60℃, nitrate concentration decreased by about 3 μM at pH 2-5, that is, pH dependence of nitrate volatilization was not observed. At −60℃ there is no liquid phase on the ice, thus nitrate ions cannot meet H^+, leading the small amount of nitrate volatilization. While, at −20℃, nitrate volatilization has a peak at pH 3. In general, volatilization of hydrochloric acid tends to proceed at lower pH. The volatilization of acid from ice surface progresses by combining concentrated H^+ and counter anion on the ice surface due to the freezing concentration effect. At pH 2, the too high concentration of sulfuric acid (5 mM) inhibited the freeze concentration effect, leading less nitrate volatilization. This result suggests that volatilization of nitrate as post-depositional process may progress in environment like Antarctica where nitrate is present on ice surface for a long time.

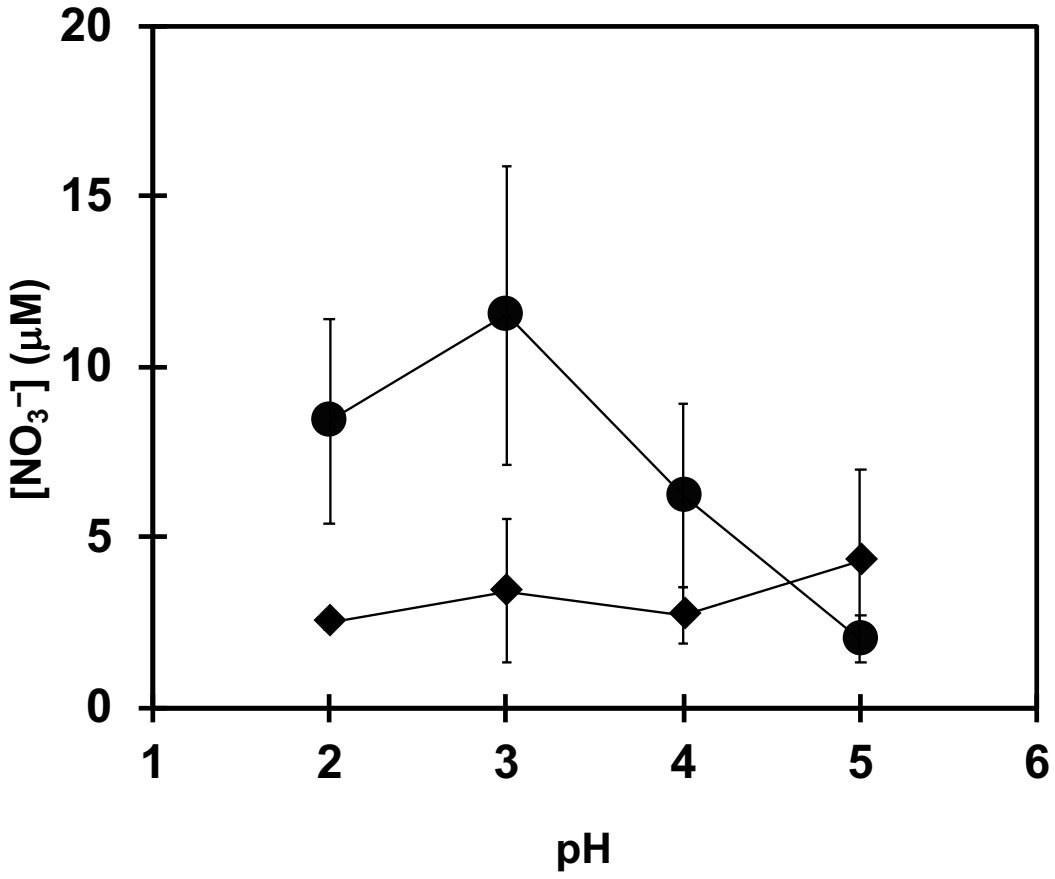

Fig. 5 Decrement of nitrate concentration (standardized by [Na^+]) by volatilization from ice surface for three weeks at −20 (circles) and −60 (diamonds) ℃.

n=3, error bar=one-σ

4.3.2 Homogenization of Snow Sample by Quartation

Table 1 shows the ion concentrations and relative standard deviations of unmixed and mixed snow samples. Except the chloride at H128, variations of all samples became small with quartation. Difference of relative standard deviation of chloride at H128 between unmixed to mixed is 3.2 which is approximately 0.1 μM. The error would come from accuracy of ion chromatograph. The quadrant method is effective for equalization

of snow.

Table 1 Ion concentrations and relative standard deviations in snow at Nagano, Rikubetsu, Gifu and H128. n=5

place	date	unmixed/ mixed	concentration			relative standard deviation		
			Cl^-	NO_3^-	Na^+	Cl^-	NO_3^-	Na^+
			(μM)			(%)		
Nagano,	17th Jan.	unmixed	54.8	12.18	*N.D.*	37.2	0.9	*N.D.*
Japan	2014	mixed	38.7	15.7	*N.D.*	17.9	1.7	*N.D.*
Rikubetsu,	1st Feb.	unmixed	27.1	28.5	*N.D.*	15.3	25.2	*N.D.*
Japan	2014	mixed	51.2	50.3	*N.D.*	5.4	12.4	*N.D.*
Gifu,	1st Feb.	unmixed	51.6	6	46.7	33.5	16.7	45.8
Japan	2015	mixed	35.3	5.5	41.3	24.6	3.6	23.5
H128,	30th Dec.	unmixed	3.9	1.7	8.4	5.1	29.4	51.2
Antarctica	2015	mixed	5.6	1.0	4.2	8.3	10	21.4

N.D.: not determined

4.3.3 Temperature in Snowpack

Fig. 6 shows temperature change in snowpack at 0, 10, 20, 30 and 40 cm depth (Fig. 6), and atmospheric temperature measured by AWS (see section 3.2.7) 2nd to 22nd January 2016. Fig. 7 shows those at 4th January 2016. Surface temperature fluctuates greatly between 3.9 to – 22.8 ℃ by sunlight heating and radiative cooling. The maximums and minimums of the days were observed around 15:00 and 2:00, respectively. At the deeper sites in snowpack, the width of the temperature change decreases. In addition, due to the adiabatic effect of snow, the time of temperature peaks at the deeper sites gradually lags from surface temperature. This width change and the time lag of temperature peaks

change thermal gradient in snowpack controlling the direction of the water vapor movement complicatedly.

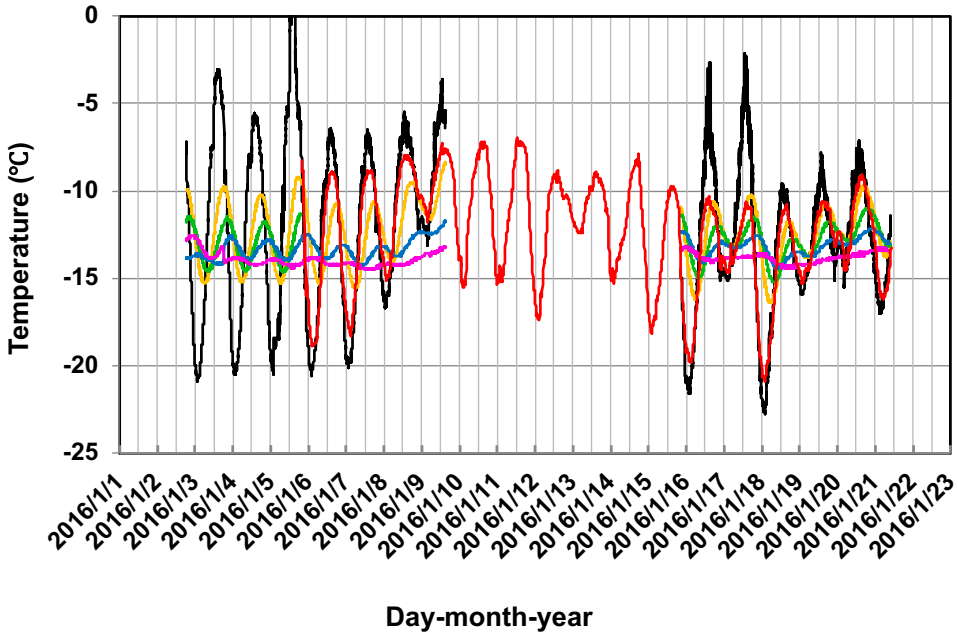

Fig. 6 Temperature in snowpack at 0 (black), 10 (yellow), 20 (green), 30 (blue) and 40 (pink) cm depth, and atmospheric temperature (red) for 1 month.

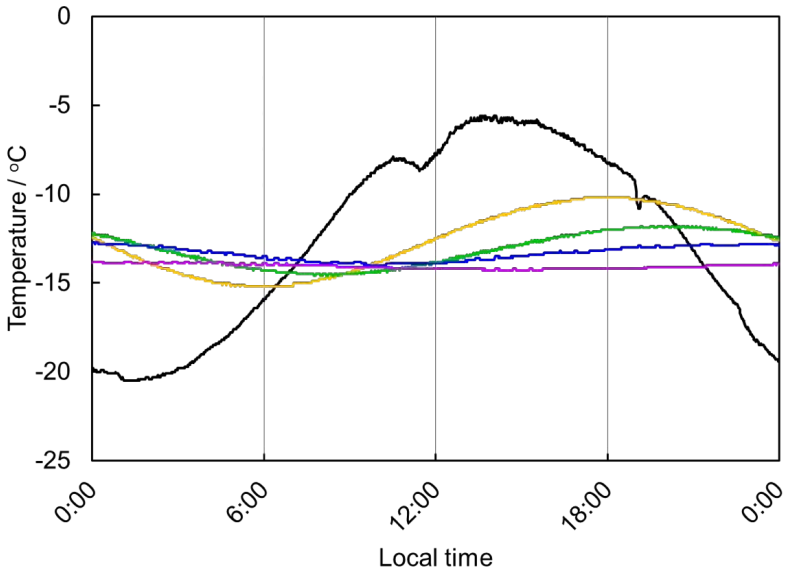

Fig. 7 Diurnal variation of *Temperature in snowpack at 0 (black), 10 (yellow), 20 (green), 30 (blue) and 40 (pink) cm depth for on 4th January 2016.*

4.3.4 Natural Snow in Antarctica

$[Na^+]$, $[Cl^-]$, $[NO_3^-]$ and $[SO_4^{2-}]$ in unmixed blank samples were 8.4 ± 4.3, 5.9 ± 0.2, 1.7 ± 0.5 and 2.0 ± 0.6 μM, respectively (n=5, error = one-σ). While, those in mixed blank samples were 4.2 ± 0.9, 5.6 ± 0.3, 1.0 ± 0.1 and 1.3 ± 0.0$_4$ μM, respectively (n=5, error = one-σ). Figs. 8 and 9 shows results of natural sample in glass tubes. Since the apparent ion concentrations change with the evaporation of water, whether the ion concentration change is due to water vapor movement or the absolute amounts of ions has changed cannot be determined. Therefore, $[Cl^-]$ and $[NO_3^-]$ are compared with $[Na^+]$ where the absolute amount does not change. Star marks in Figs 8 and 9 show $[Cl^-]$ / $[Na^+]$ or $[NO_3^-]$ / $[Na^+]$ of mixed blank sample. If the ion concentration change is only due to water vapor movement, all the plots should be on the straight line. In addition, if a plot is on the right side of this line, it indicates that $[Cl^-]$ or $[NO_3^-]$ is decreasing by post-depositional process. Conversely, if a plot is on the right side of this line, it indicates that $[Cl^-]$ or $[NO_3^-]$ is increasing by post-depositional process or deposition from atmosphere. Under the conditions of OPEN and COVERED, chloride ions were lost in surface snow (0-5 and 5-10 cm depth). There is significant difference between $[Cl^-]$ / $[Na^+]$ of surface snow sample (0-5, 5-10 cm depth) (p=0.05). While, $[Cl^-]$ / $[Na^+]$ under DARK condition was stable. Similar to chloride results, nitrate was lost in surface snow (0-5 and 5-10 cm depth) under OPEN and COVERD condition. There is also significant difference between $[NO_3^-]$ / $[Na^+]$ of surface snow sample (0-5, 5-10 cm depth) (p=0.05). Because most plots are on the right side of blank under all conditions, water evaporation occurs in the glass tube. Due to this moisture vapor movement, surface snow becomes more dry condition which

may lead volatilization of HCl or other organic acids. Even under DARK conditions, it is dried by water vapor movement, but all the plots are on the blank line. In other words, HCl emission for atmosphere has not progressed under DARK conditions. The reason why HCl emission into the atmosphere did not proceed under DARK condition may be temperature gradient in the glass tube. Under the DARK condition, aluminum tape wrapped around the glass tubes and the beakers absorbed the sunlight, possibly the temperature was rising. Therefore, there is a possibility that this difference in temperature state may influence the behavior of chloride ion, but details are not clear. On the other hand, nitrate ions also behave similar to chloride ions, however the reason is different. The main cause of nitrate ion loss is photolysis. Therefore, the nitrate was stable under the DARK condition because the photolysis reaction did not proceed. Furthermore, under the OPEN and COVERED conditions, the plot deeper than 10 cm is also on the right side of the line. Therefore, nitrate photolysis may proceed even deeper than 10 cm depth in snowpack. Moreover, under the OPEN and COVERED conditions, the glass tube prevents the penetration of UV from the side, thus more nitrate has disappeared with photolysis. Although nitrate photolysis may produce NO_2^-, it was not detected. Therefore, all nitrogen oxides generated by nitrate photolysis are released into the atmosphere as gases.

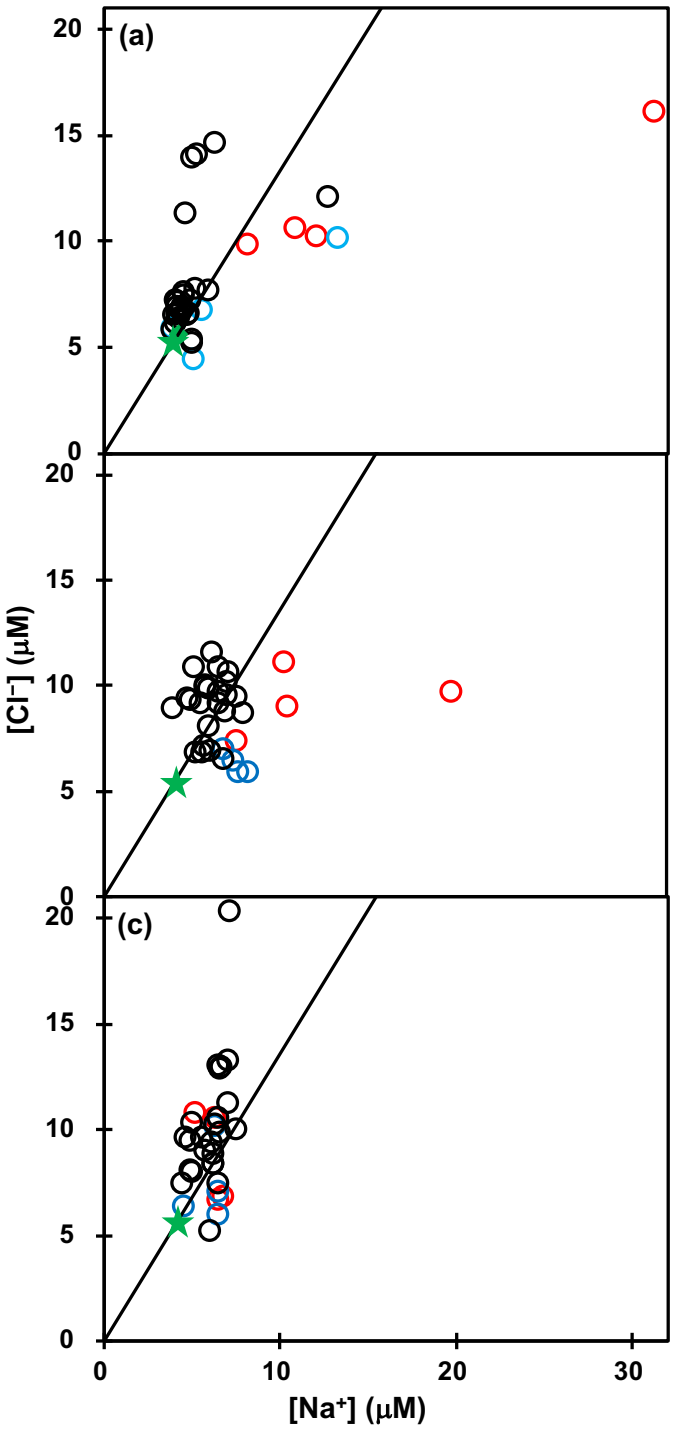

Fig. 8 [Cl^-] in natural sample comparison with [Na^+]. Red: 0-5 cm; Blue: 5-10 cm; Black: 10-20, 20-30 and 30-40 cm, and Star: mixed blank. The slope of the line is [Cl^-] /[Na^+] of mixed blank. (a): OPEN; (b): COVERED; (c): DARK.

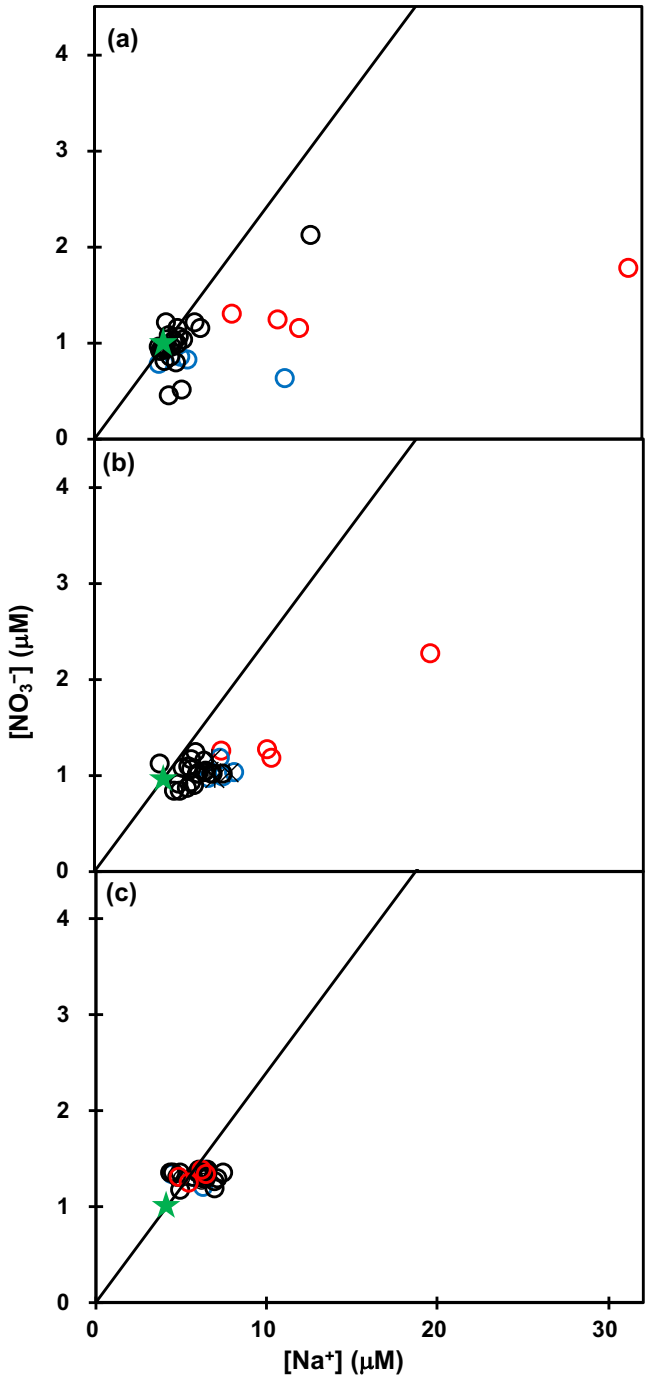

Fig. 9 [NO_3^-] in natural sample comparison with [Na^+]. Red: 0-5 cm; Blue: 5-10 cm; Black: 10-20, 20-30 and 30-40 cm, and Star: mixed blank. The slope of the line is [NO_3^-] /[Na^+]of mixed blank. (a): OPEN; (b): COVERED; (c): DARK.

4.3.5 Amended Sample in Antarctica

[Na^+], [NH_4^+], [Cl^-] and [NO_3^-] in mixed amended blank samples were 322.1 ± 23.3, 161.1 ± 12.5, 305.2 ± 14.0 and 148.63 ± 7.4 μM, respectively. Similar to the results of natural sample, chloride and nitrate were lost from surface (0-5 cm) under OPEN and COVERED condition Cl^- and NO_3^- behavior in each condition are almost the same as natural samples (Figs. 10 and 11). However, under the OPEN and COVERED conditions, the photolysis reaction has not progressed at a depth deeper than 5 cm. Due to the high nitrate concentration, nitrate on the surface absorbed most of UV which leaded that UV could not penetrate deeply.

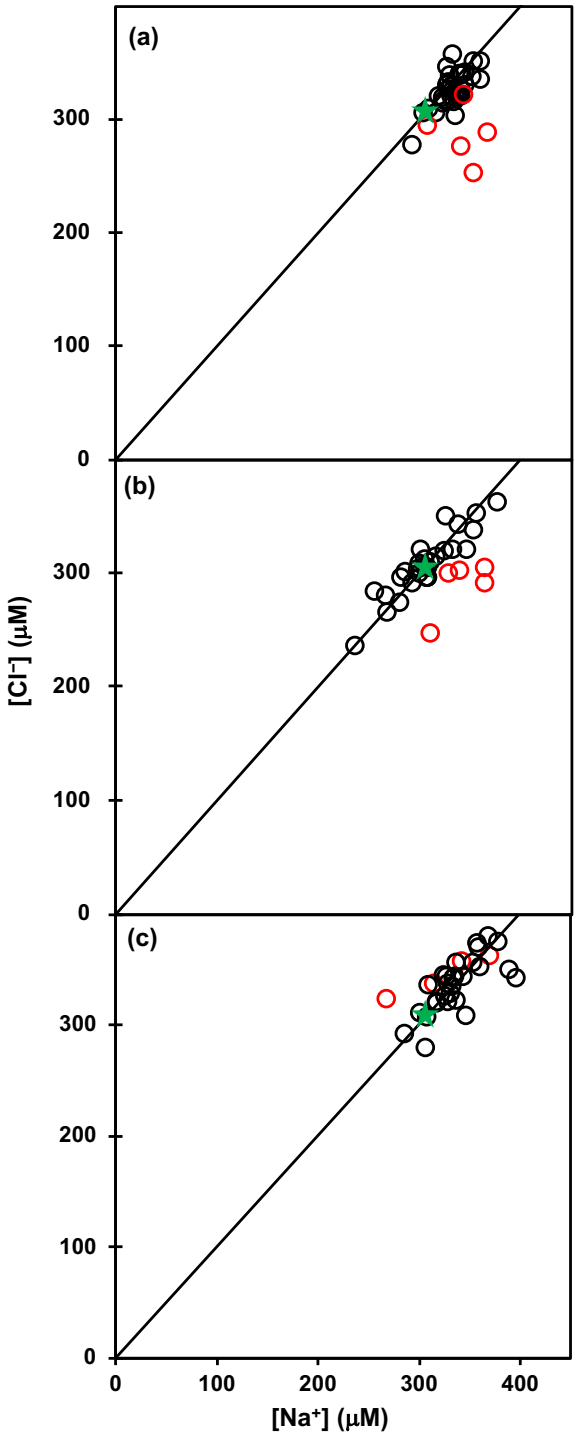

Fig. 10 [Cl^-] in amended sample comparison with [Na^+]. Red: 0-5 cm; Blue: 5-10 cm; Black: 10-20, 20-30 and 30-40 cm, and Star: mixed blank. The slope of the line is [Cl^-] /[Na^+] of amended mixed blank. (a): OPEN; (b): COVERED; (c): DARK.

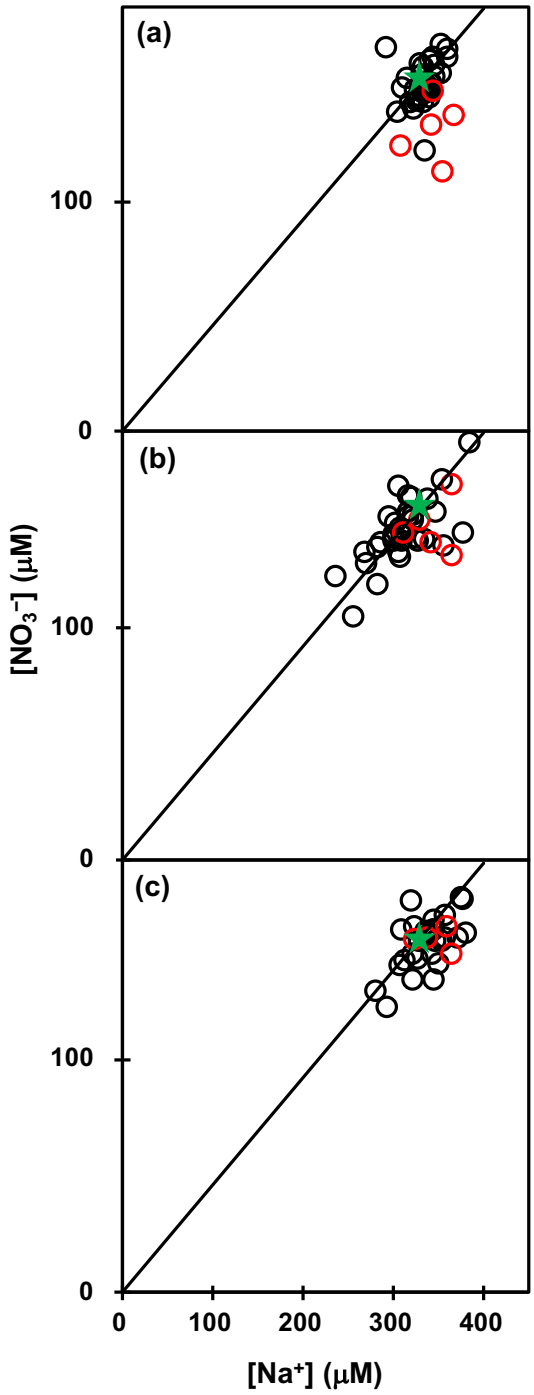

Fig. 11 [NO_3^-] in amended sample comparison with [Na^+]. Red: 0-5 cm; Black: 5-10 cm; 10-20, 20-30 and 30-40 cm, and Star: mixed blank. The slope of the line is [NO_3^-] /[Na^+] of mixed blank. (a): OPEN; (b): COVERED; (c): DARK.

4.3.6 Light Intensity in Snowpack

Fig. 12 shows depth dependence of solar spectrum. In the deep part of the snowpack, the light intensity weakens. Comparing the maximum value of the light intensity at 10 cm depth and 100 cm depth, it is about a quarter of light intensity at 100 cm to at 10 cm. Also, it can be seen that the shape of the spectrum is changing. The reason why the spectra of depths 50 cm and 75 cm intersect at around 480 nm is that these two observation times are about two hours apart. Fig. 13 shows the standardized values of each spectrum using value of 500 nm. Compared to the reference as direct solar spectrum, the relative intensity on the short wavelength increases at the deeper depth. In other words, long wavelength light is absorbed in water molecules, however short wavelength light may penetrate in deeper snowpack. Fig. 14 shows the light intensity at 310, 400, 500 and 600 nm at each depth. The intensity of 310 nm light does not change much from 10 to 100 cm depth. On the other hand, the longer wavelength light intensities clearly decrease at deeper site of the snowpack. 310 nm is an important wavelength for nitrate photolysis. Since the light of this wavelength has reached 100 cm depth, the nitrate photolysis reaction progresses even in the vicinity of the depth of 100 cm. It is no wonder that the reaction proceeds at a depth of 100 cm, considering that the reaction has progressed to a depth of 40 cm even under weak light conditions with the side glass wall as obstacle. These results are the first data obtained in field observation of light intensity in snowpack.

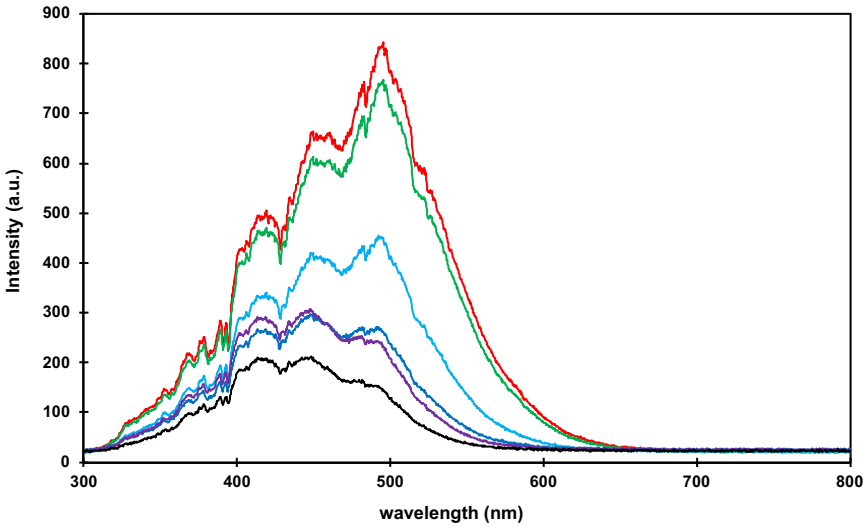

Fig. 12 Depth dependence of solar spectrum in snowpack. At 10 (red), 20 (green), 30 (light blue), 50 (navy blue), 75 (purple) and 100 cm depth (black). Measured on 12:00-16:00 p.m. on 14th January 2015.

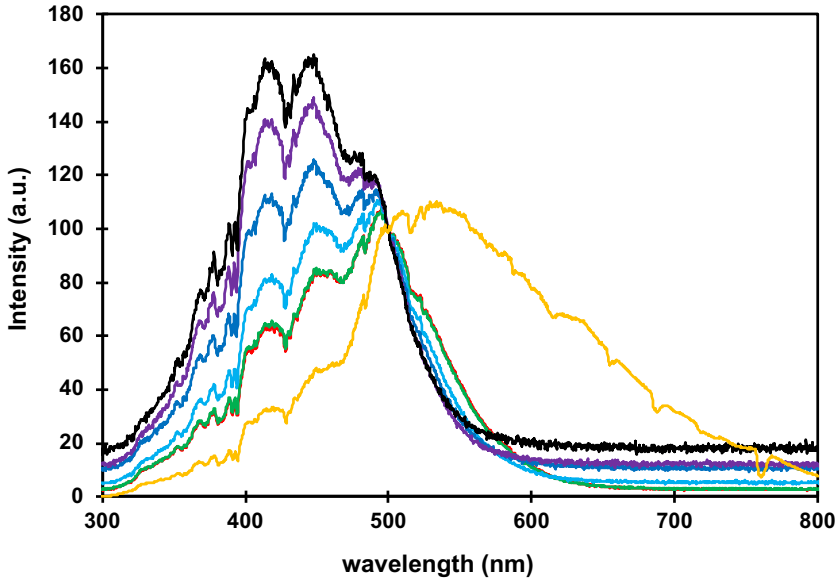

Fig. 13 Depth dependence of solar spectrum standardized at 500 nm in snowpack. At 10 (red), 20 (green), 30 (light blue), 50 (navy blue), 75 (purple),100 cm depth (black). Orange line is reference. Measured on 12:00-16:00 p.m. on 14th January 2015.

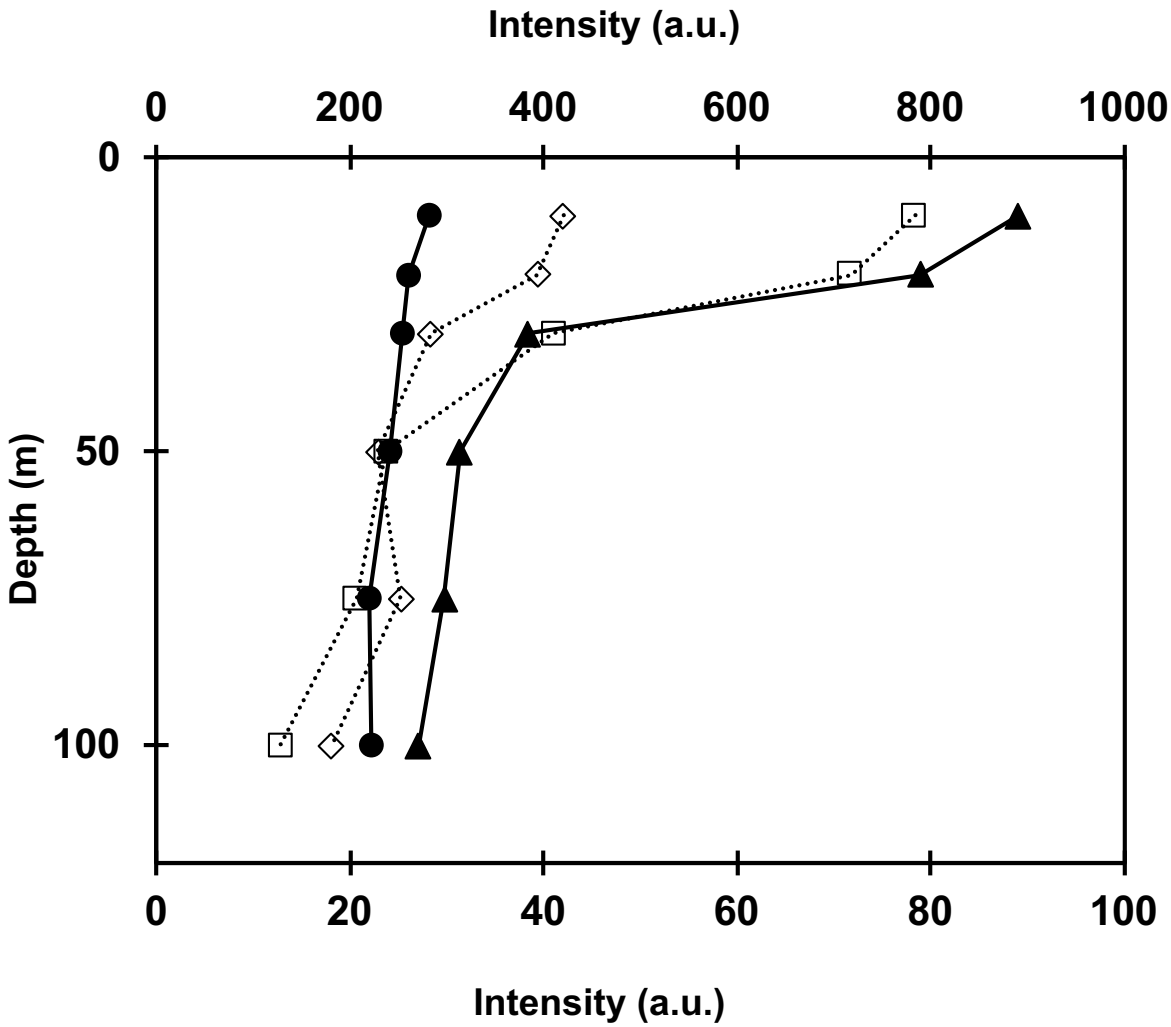

Fig. 14 Depth profile of light intensity at 310 (circles, lower axis), 400 (diamonds, upper axis), 500 (squares, upper axis) and 600 nm (triangles, lower axis). Measured on 12:00-16:00 p.m. on 14th January 2015.

4.3.7 Estimation for Post Depositional Loss of Chloride and Nitrate

The density of snow in the glass tube was approximately 0.5 g cm^{-3}, then chloride and nitrate loss from each depth can be calculated. Fig. 15 shows the chloride and nitrate change, and [Na^+] under OPEN condition after four weeks. As [Na^+] of 2.5 cm depth is

relatively high, it turns out that water was evaporated. The change in [Cl^-] is small in the part where water evaporates, however the concentration is rising in the other deeper sites. In other words, HCl deposited to the snowpack surface would gradually move to a deeper site in snowpack. Cl^- moved through firn as HCl gas or in the grain boundary in ice as Cl^-. In either way, 100% of the chloride moving through snow indicates the possibility that other chemical species may also move in snowpack. On the other hand, nitrate near the surface decreased more than 50 %. There is no report that 50 % of nitrate has disappeared from the snowpack on the Antarctic coastal site. It is reported that nearly 90% of nitrate loss by photolysis in the Antarctic inland such as Dome Fuji (Noro *et al.*, 2018), thus the progress of nitrate photolysis may be also remarkable in the coastal site. Furthermore, nearly 20 % of nitrate disappears even at a depth of 40 cm. This result can be explained by light of 310 nm penetrating deeper site in snowpack as we mentioned. The most nitrate remaining at 25 cm depth is because the light is obstructed by the glass wall. Thus the nitrate loss was under estimated. In the lower part of the glass tube, the reaction proceeded by the light from lower site.

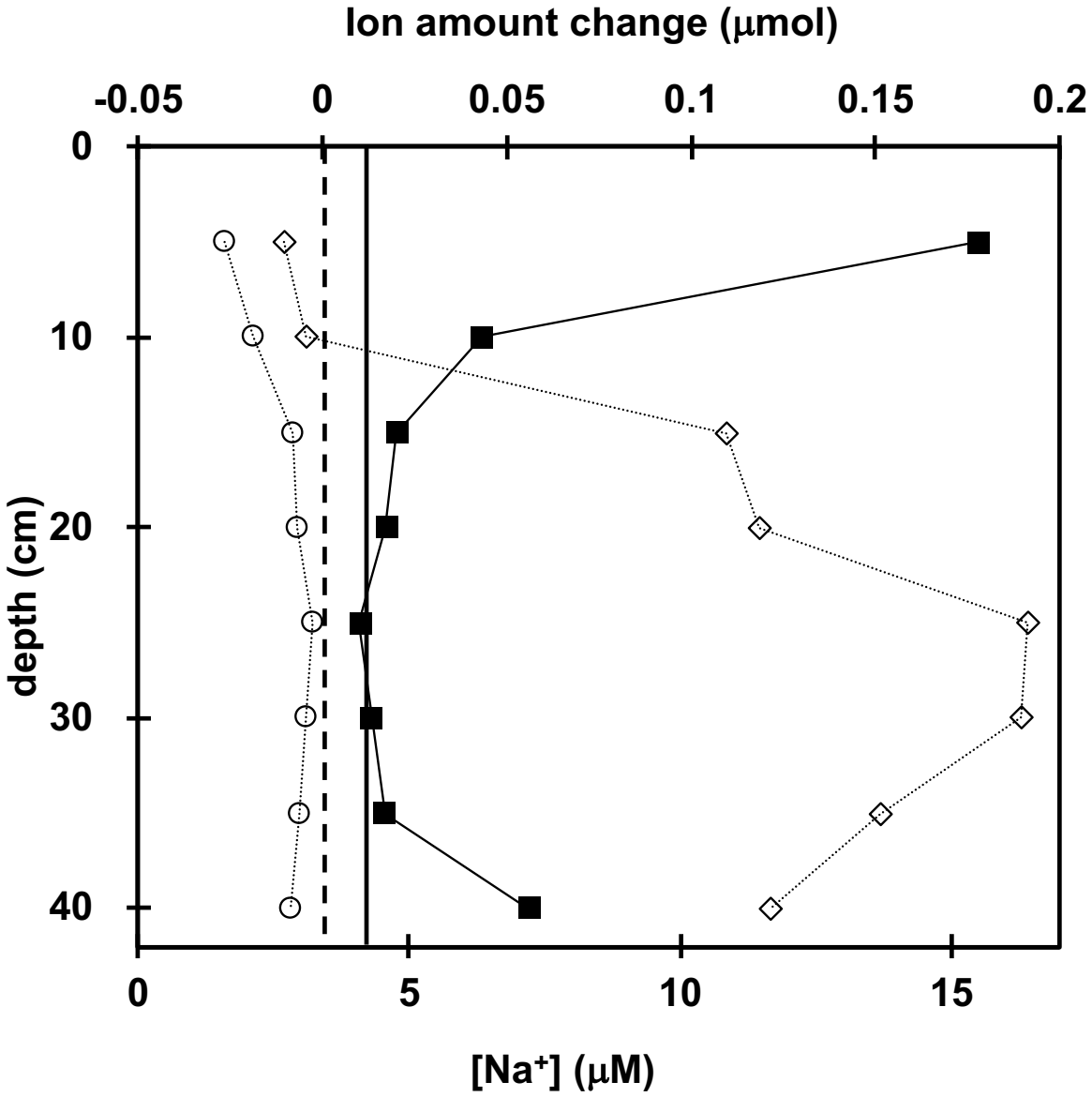

Fig. 15 Depth profile of Cl^- (diamonsd) and NO_3^- (circles) loss, and [Na^+] (square).

Solid line: initial value of [Na^+].

4.4 Conclusion

A glass tube experiment using Antarctic environment as a laboratory was

conducted at H128 (69°23.584S°, 41°33.712E°) at about 100 km from Syowa Station in eastern Dronning Maud Land, East Antarctica during the 57th Japanese Antarctic Research Expedition (JARE57) for December 2015 to February 2016. As a result, it was found that the chloride moved to the deeper site in snowpack due to the influence of water vapor movement. Nitrate had disappeared from the surface snow more than 50% by photolysis. Furthermore, near 20% nitrate had disappeared even at the depth of 40 cm. There has been no report of evidence of such chloride ion movement in snowpack and remarkable nitrate loss in the Antarctic coastal site. These results add new findings to Antarctic geochemical cycle.

References

Blunier, T., Floch, G. L., Jacobi, H.-W. and Quansah, E. (2005). Isotopic view on nitrate loss in Antarctic surface snow. *Geophys. Res. Lett., 32*(13), L13501. doi:10.1029/2005GL023011

Dibb, J. E., Talbot, R. W., Munger, J. W., Jacob, D. J. and Fan, S. M. (1998). Air-snow exchange of HNO_3 and NOy at Summit, Greenland. *J. Geophys. Res.-Atmos., 103*(D3), 3475-3486. doi:10.1029/97JD03132

Frey, M. M., Savarino, J., Morin, S., Erbland, J. and Martins, J. M. F. (2009). Photolysis imprint in the nitrate stable isotope signal in snow and atmosphere of East Antarctica and implications for reactive nitrogen cycling. *Atmos. Chem. Phys., 9*(22), 8681-8696. doi:10.5194/acp-9-8681-2009

Grannas, A. M., Hockaday, W. C., Hatcher, P. G., Thompson, L. G. and Mosley-Thompson, E. (2006). New revelations on the nature of organic matter in ice cores. *J. Geophys. Res.-Atmos., 111*(D4), D04304. doi:10.1029/2005JD006251

Honrath, R. E., Peterson, M. C., Guo, S., Dibb, J. E., Shepson, P. B. and Campbell, B. (1999). Evidence of NOx production within or upon ice particles in the Greenland snowpack. *Geophys. Res. Lett., 26*(6), 695-698. doi:10.1029/1999GL900077

Jacobi, H.-W. and Hilker, B. (2007). A mechanism for the photochemical transformation of nitrate in snow. *J. Photoch. Photobio. A, 185*(2), 371-382. doi:https://doi.org/10.1016/j.jphotochem.2006.06.039

Jones, A. E., Weller, R., Anderson, P. S., Jacobi, H. W., Wolff, E. W., Schrems, O. and

Miller, H. (2001). Measurements of NOx emissions from the Antarctic snowpack. *Geophys. Res. Lett., 28*(8), 1499-1502. doi:10.1029/2000GL011956

Mack, J. and Bolton, J. (1999). *Photochemistry of nitrite and nitrate in aqueous solution: A review* (128), 1-13.

Meusinger, C., Berhanu, T. A., Erbland, J., Savarino, J. and Johnson, M. S. (2014). Laboratory study of nitrate photolysis in Antarctic snow. I. Observed quantum yield, domain of photolysis, and secondary chemistry. *J. Chem. Phys., 140*(24), 244305. doi:10.1063/1.4882898

Röthlisberger, R., Hutterli, M. A., Sommer, S., Wolff, E. W. and Mulvaney, R. (2000). Factors controlling nitrate in ice cores: Evidence from the Dome C deep ice core. *Journal of Geophysical Research: Atmospheres*, *105*(D16), 20565-20572. doi:10.1029/2000JD900264

Sato, K., Takenaka, N., Bandow, H. and Maeda, Y. (2008). Evaporation Loss of Dissolved Volatile Substances from Ice Surfaces. *Phys. Chem. A, 112*(33), 7600-7607. doi:10.1021/jp075551r

Traversi, R., Usoskin, I. G., Solanki, S. K., Becagli, S., Frezzotti, M., Severi, M., Stenni, B. and Udisti, R. (2012). Nitrate in Polar Ice: A New Tracer of Solar Variability. *Solar Physics*, *280*(1), 237-254. doi:10.1007/s11207-012-0060-3

Soil microbial experiment method (1977), Yokendo, Japan. *in Japanese.*

Chapter 5: Conclusions and Future Research

The works presented in this thesis focus on the nitrogen oxides cycle in Antarctica. In particular, the mechanism of nitrate photolysis in snowpack and its products were investigated.

In chapter 1, background of this thesis is summarized.

In chapter 2, spatial variations in NO_3^- isotopic compositions from coastal to inland sites in eastern Dronning Maud Land, East Antarctica was reported. Although the NO_3^- concentrations of surface snow between coastal and inland sites ranged from 40.0 to 130.8 μg L^{-1}, without explicit trends with latitude, the $\delta^{15}N(NO_3^-)$ values in the surface snow increased along the traverse from coastal sites to inland sites, ranging from −19.4 to 165.5 ‰. Based on a Rayleigh model, the remaining nitrate mass fraction was calculated to vary from 5 to 32 % at sites DF1, NDF, Plateau S, S80, Fuji Pass, and DF2. This suggests that at these inland sites, between 68 and 95 % of nitrate was removed via UV photolysis of the snowpack. In contrast, the $\delta^{15}N(NO_3^-)$ values at coastal sites were lower than$\delta^{15}N$ values of stratospheric nitrate, exhibiting a large variation in nitrate concentrations but a small variation in $\delta^{15}N(NO_3^-)$ values. This indicates that the horizontal redistribution via advective transport of nitrate has an important effect on nitrate concentrations in surface snow at coastal sites. The relationship between the isotopic values ($\delta^{15}N(NO_3^-)$ and $\Delta^{17}O(NO_3^-)$) and snow accumulation rate is consistent with previous traverses across East Antarctica, implying that UV-driven post-depositional loss and horizontal redistribution occur similarly throughout East Antarctica.

In chapter 3, observation data of background NO_y concentration, NO_y flux from snowpack surface and depth profile of HONO in the snowpack in the coastal site in the

Antarctica were provided. NO_2 was not detected both in the atmosphere and from snowpack. We concluded that the difference between previous data and our data was due to the difference in measuring equipment. Previous studies that measured NO_2 using the chemiluminescence method may possibly overestimate NO_2. Our results suggested that the primary product from nitrate photolysis is HONO and the secondary product is NO. In addition, from the results of the passive sampler and flux from dark chamber, nitrate photolysis would be progressed in the deep snow about 1 m.

In chapter 4, a glass tube experiment using Antarctic environment as a laboratory was conducted at H128 ($69^{\circ}23.584S^{\circ}$, $41^{\circ}33.712E^{\circ}$) at about 100 km from Showa Station in eastern Dronning Maud Land, East Antarctica during the 57^{th} Japanese Antarctic Research Expedition (JARE57) for December 2015 to February 2016. As a result, it was found that the chloride moved to the deeper site in snowpack due to the influence of water vapor movement. Nitrate had disappeared from the surface snow more than 50 % by photolysis. Furthermore, near 20 % nitrate had disappeared even at the depth of 40 cm. There has been no report of evidence of such chloride ion movement in snowpack and remarkable nitrate loss in the Antarctic coastal site. These results add new findings to Antarctic geochemical cycle.

In chapter 5, summary of this doctoral thesis and a prospect for the future research is written.

It is believed that the results will contribute significantly to the understanding of nitrogen oxides cycle in Antarctica. In particular, the mechanism of nitrate photolysis in snowpack and its products were investigated. With the detailed behavior of nitrate within

the snowpack in Antarctica, paleo climate and atmospheric research using ice cores will be accelerated. While, new findings make new questions. Therefore, I would like to propose the following research for future studies:

>HONO measurement at Antarctic inland such as Dome Fuji. It is possible that the difference between coastal to inland in weather condition (*e.g.* temperature and humidity) would affect the nitrate photolysis in snowpack. In order to know the detailed behavior of nitrogen oxides, it is necessary to know the region dependency.

> Grasp of wide area distribution of nitrogen oxide by passive sampler. Multipoint measurement is difficult in Antarctica. To that problem passive samplers will show great power.

>Narrow area snow sampling for $\Delta^{17}O(NO_3^-)$ analysis. There are many unclear points in the behavior of $\Delta^{17}O(NO_3^-)$. A combination of intensive observation in a narrow range and observation in a wide area is needed.

> Contribution of nitrate volatilization. The influence of volatilization cannot be analyzed by isotopic observation. Its contribution is said to be small, but its details are unknown.

>Influence of nitrate photolysis on organic matter. Nitrate photolysis produces oxidants. It should have influence for life time of organic matters.

List of Publications

No.	論文題目	著者名	発表誌名	本論文との対応
1	Isotopic constrains on post-depositional processing of snow nitrate in eastern Dronning Maud Land, East Antarctica	K. Noro S. Hattori R. Uemura K. Fukui M. Hirabayashi K. Kawamura H. Motoyama N. Takenaka N. Yoshida	Geochem. J., accepted for publication.	第２章
2	NO_x flux from snow surface and the depth profile of HONO in snow pack in eastern Dronning Maud Land, East Antarctica	K. Noro M. Arai T. Sakurai K. Kawamura H. Motoyama N. Takenaka	Bull. Glaciol. Res., submitted.	第３章
3	Photolysis and sublimation as post-depositional loss of nitrate and chloride in snow	K. Noro M. Arai T. Sakurai K. Kawamura H. Motoyama N. Takenaka	International Journal of Science, submitted.	第４章

Acknowledgements

Firstly, I would like to express me deep gratitude to my supervisor, Norimichi Takenaka, for his guidance and support during my B4 to Ph.D life for six years. He invited me to 57th Japan Antarctic Research Expedition which should be a highlight in my life. He was surprisingly persistent and did not quit educating me for foolishness. Of course, without him, I did not complete even master course.

I would like to express my sincere thank to Prof. Masaya Matsuoka and Hideaki Hisamoto for their precious time reviewing my work. This thesis is greatly improved from their valuable comment and advice.

I would like to express my sincere thank to Dr. Shohei Hattori. Despite belonging at Tokyo Institute of Technology, he instructed me as a student of Osaka Prefecture University with great enthusiasm. Without his help, I could not complete my Ph.D.

I would like to express my heartfelt gratitude to JARE57 members, especially “inland team”. We spent wonderful and scientific time together.

I would like to express my special thank to Prof. Teruo Aoki and Dr. Naohiko Hirasawa. They helped and guided me to measure light intensity in snowpack.

I would like to thank a program for Leading Graduated School the Graduate Course of System-inspired Leaders in Material Science (SiMS program) for providing me with its prestigious scholarship to purse higher education. They also supported me to study in Antarctica, US and Vietnam.

I would like to thank my lab-mates at OPU Laboratory of Environmental Materials

Chemistry, especially Vietnamese friends. Their attitude and effort always encouraged me. They are my best friends and my best foreign language teachers.

I would like to thank my girlfriend Mayu Shimono. Her contribution was significant. She has good skill for cooking, very funny personality, and talent for singing. I never got tired of staying with you.

I would like to thank my favorite writers: Haruki Murakami, Kazuo Ishiguro, Truman Capote, Raymond Chandler, Gen-ichiro Takahashi, Garcia Marquez, John Irving and my favorite rock bands: RED HOT CHILI PEPPERS and Rancid. Their amazing performance and their works fill my heart. They make me relax even though during blizzard in Antarctica.

Finally, I would like to express my gratitude to my parents and entire families. They never said me “No”. They always supported me secretly. To not show off your efforts is a rare virtue. I am happy with such great parents who kept waiting silently.

Kazushi NORO